The Annual Cycle of Monthly Correlations between Station Mean Air Temperature and Sunshine Receipt over the United States

A Senior Honors Thesis

Presented in Partial Fulfillment of the Requirements for
Graduation *with distinction* in Atmospheric Science in the Undergraduate Colleges
of The Ohio State University

by

Todd R. Jones

The Ohio State University
May 2006

Project Advisor: Professor Jeffery C. Rogers, Department of Geography

Abstract

The strong positive relationship between global air temperature measurements and solar irradiance values has been recognized by multiple researchers, and some have also noted the near 1-to-1 relationship between solar irradiance and sunshine duration measurements. This investigation applies these findings by combining the two relationships in order to understand links between average monthly air temperatures and average monthly sunshine duration as a percentage of maximum possible using weather station data from 113 sites across the United States. The monthly time scale data produce clear annual cycles in linear correlation values that vary in both sign and magnitude throughout the year, generally having large positive correlations in the summer and relatively large negative correlations in the winter months. Also, distinct spatial patterns of correlation variability within these annual cycles have been observed by using principal component analysis. Three clearly different regional correlation patterns were found; the largest encompasses the northeast, the Midwest, and the northern Great Plains; another lies directly to the south along the mid-Atlantic coast, extending inland to the Mississippi; and a third lies along the Gulf Coast. In addition, it was found that the relationship between air temperature and sunshine duration may be quadratic rather than linear. These regional patterns may have some application in aspects of applied meteorology and atmospheric science research in the areas of forecasting and atmospheric modeling, as well as in the understanding of how temperatures in specific regions will respond in light of global brightening.

1. Introduction

Relationships between solar irradiance and air temperature have been the subject of much study and attention in recent years, as understanding this linkage is an integral part of creating sound scientific research on issues such as temporal trends in global temperature, the parameterization of radiation in numerical modeling, and numerous other facets of atmospheric science. There is evidence in support of the idea that changes in solar irradiance have, in effect, caused direct changes in global temperatures measured at the surface (Balling and Roy 2005). Specifically, Balling and Roy (2005) show a linear Pearson correlation coefficient of 0.51 for temperature anomalies and solar irradiance over the years 1910-2003. In recent years, however, this relationship has weakened due to anthropogenic forcings on the climate system in the form of greenhouse gases and other potential feedback mechanisms involving aerosols and water vapor (Meehl *et al.* 2003; Gleisner and Thejil 2003). Fortunately, the scope of this study is much more heavily influenced by the time period prior to the mid-late 1970's, which is the time when the deviation in the relationship begins to occur.

Sunshine duration measurements can be reasonably used as a proxy for solar radiation measurements, the accuracy and abundance of which have been quite lacking in the United States (Stanhill and Cohen 2005). Stanhill and Cohen found that sunshine duration and global radiation are linearly correlated, with $r = 0.926$, indicating the possibility of using the two measures quasi-interchangeably. In fact, Stanhill and Cohen (2005) also report that information obtained from sunshine duration recorders has been used "widely and successfully" in place of solar radiation data for 75 years. Their study

involved annual sunshine duration measurements, which prior to that point had not been used in place of solar radiation measurements.

In this study, the relationships between temperature and solar irradiance and between solar irradiance and sunshine duration have been, in essence, combined in order to look at the relationship between sunshine duration percentage of maximum possible, in the form of monthly means, and air temperatures, also in the form of monthly means. A study involving these two measurements is not known to have been conducted to date. Since this is the case, this study provides a rudimentary analysis of these data, involving correlations, both linear and quadratic, between monthly air temperatures and sunshine duration as a percentage of maximum and a principal component analysis of the correlation matrices that determine the spatial patterns in the station correlation results and variations in the annual sequence of these correlations.

2. Measurements

Sunshine duration measurements began in organized fashion in 1891 using a modified version of the Jordan photographic recorder, invented in 1838, that "burned" marks onto sensitized sheets in the presence of direct sunlight. These early measurements were recorded at a mere 20 U.S. Weather Bureau stations. By 1908, the Jordan recorder had been fully replaced by the Maring-Marvin thermometric sunshine switch, and the size of the observing network had more than doubled (Stanhill and Cohen 2005; Quinlan 1985). To measure the presence of sunshine, this device used the principle of differential energy absorption between black and clear bulbs of two thermometers, connected by a straight tube that were protected from the effects of air temperature by

being encased in an evacuated glass chamber. As mercury rose away from the black bulb in the presence of direct sunlight, it completed an electrical circuit and allowed the recorder to begin recording. The third and final instrument to be collectively implemented was the Foster Photoelectric Sunshine Switch, which began operation in 1953. This device consists of two photoelectric cells, one shaded and the other open. The electrical potential created by the sun's light on the unshielded cell turned on the device at a certain threshold value, which is related to the amount of direct sunlight required to cast a shadow. This permits measurement during times of thin cirrus but not during thick cirrus (Angell *et al.* 1984). The other cell was shaded in order to measure diffuse radiation. Stanhill and Cohen (2005) indicate that the Foster Switch is currently in operation. The full sunshine duration dataset was compiled by Steurer and Karl (1991), but the dataset used terminates in 1987.

With the noted shifts in measurement techniques, question arises as to the accuracy and homogeneity of the long-term dataset. Stanhill and Cohen (2005) reached the conclusion that the replacement of the photographic method with the thermometric method had a "minor and nonsignificant effect…[, and that]…even at the site showing the largest change, [the effect] was not statistically significant." The change in duration measurements was 1.9% over the time of the instrumentation change compared to the +3.8% to -10% intersite variation during the same change period. A similar conclusion was reached for the change from the thermometric recorders to the photoelectric recorders. Though their analysis of this effect dealt with only annual sunshine duration, the assumption was made that the same is true for the monthly sunshine duration data used here, after preliminary analyses found nothing of note when analyzing the data for

shifts in the mean values through time using a shift detection add-on in the Microsoft Excel (Rodionov, 2004).

Temperature measurements were obtained online from the Midwestern Regional Climate Center's Midwestern Climate Information System (MICIS). The data obtained were originally recorded at U.S. Weather Bureau or Service Offices or airport weather stations near the corresponding sunshine duration measurement instrument, and were in the form of monthly averages in degrees Fahrenheit. Every effort was made to procure continuous datasets of considerable length for each site in the study, but in some instances, information from Weather Bureaus and Service Offices and other nearby sources had to be combined at arbitrary points in time due to overlaps and discontinuities to achieve this goal. These junctions were only performed where no significant steps, representing changes in the value of average monthly air temperature with time, are created in the full time series. In cases where significant steps would occur, the series that corresponded to longer concurrent available sunshine duration data was selected over the shorter, in order to give a more representative account of a particular site.

3. Methods

a) Data Preparation

As observing stations were slowly aggregated, not all stations in the study have time series of the same length. Available sunshine duration percentage data ended in 1987, and all sites considered in the study have time series ending in that year. The two datasets were paired to create the longest possible series of comparable information. This may have introduced some bias into the analyses in that some sites are not entirely

comparable to others in terms of their overall averages. For example, in Spokane sunshine data are available 1897-1987, and air temperature data are available 1890-2006. Thus, its overall comparable time series was 1897-1987. In Seattle, sunshine data exists from 1897 to 1987, and air temperatures are available from 1948 to 2006. Its overall comparable time series was 1948-1987. Averages of these two sites encompass obviously differentiated information and may not be well compared due to bias in the shorter time series toward the period from the 1950s to the 1970s, which was significantly cooler than the time prior that was factored into the longer time series.

Further, it is important to note that no series was shorter than 1955-1987 and that sites with a sufficiently long sunshine duration time series were not considered if the corresponding temperature series had gaps beyond a few years that could not be accounted for with data from a nearby location. Also, monthly averages for both sunshine duration and temperature that were missing for periods no longer than 4 months were replaced with the average value for that month for that site over the entire available series regardless of the length of the corresponding series. Using these methods, 113 of a possible 121 sites in the United States were found suitable for analysis. The sites analyzed in this study are listed in Table 1 along with each site's earliest year for comparison of its monthly average sunshine duration percentage and monthly average air temperature datasets.

The eight sites that were not included in the analysis were Savannah, GA, Trenton, NJ, Wilkes-Barre, PA, New Haven, CT, Port Arthur, TX, Dallas/Fort Worth, TX, Phoenix, AZ, and Sacramento, CA. Reasons for exclusion were purely technical with respect to their temperature dataset availability. Some were highly discontinuous, others

had records that were deemed to be too short for analysis, and some datasets ended far before 1987, which made them also too short to be analyzed. In each case, no suitable nearby replacement could be obtained. Unfortunately, half of these exclusions add to a void of information, particularly in areas of Texas and in the Southwest (Phoenix and Sacramento), where the total number of sites was already relatively limited. Areas near the other four excluded sites, those in the eastern part of the United States, have a multitude of surrounding sites, which makes the loss of information in those areas have less of an obvious impact.

b) Correlations

In order to gain perspective on the relationship between average monthly sunshine duration as a percentage of that possible and average monthly temperature, correlations and regressions were performed on a monthly basis for all 113 sites for station periods of record. Equations of the linear regression lines produced by this study follow the form:

$$y = ax + b \qquad (1)$$

where y acts as the dependent variable, x acts as the independent variable, a is the slope of the trend through the data shown in the scatterplot, and b is the regression constant and y-intercept of the regression line. To further examine the relationship between average monthly sunshine duration and average monthly temperature, quadratic regressions were also performed for all 113 sites for their periods of record. The purpose of this part of the analysis was to evaluate scatterplots and determine if the best fit through the data is linear or a second order polynomial (quadratic) expression. Further, the quadratic regression aids in determining whether a relationship that is better fit to a quadratic function than a

linear function follows a concave up or concave down curvilinear line following the second order polynomial equation:

$$y = ax^2 + bx + c \qquad (2)$$

where y acts as the dependent variable, x acts as the independent variable, a is a regression coefficient characterizing the curvature of the parabolic function in that when it is positive, it is concave up, and when it is negative it is concave down and also the width of the parabola in that when it is of very low magnitude, the parabola is expanded in the x-direction, attaining the form of a straight line when equal to zero, b is a regression coefficient characterizing the placement of the curve in space, and c is a constant representing the y-intercept of the function.

Pearson product moment correlation is used as a measure of the direction and strength of a linear relationship between two variables, and is calculated as a value, r, ranging from -1 to +1, where -1 is a strong negative relationship, +1 is a strong positive relationship, and 0 represents no relationship (Moore and McCabe 2006). The correlation coefficient, r, was calculated using the following equation:

$$r = (1 / n - 1) \sum ((x_i - \bar{x} / s_x) (y_i - \bar{y} / s_y)) \qquad (3)$$

where the means and standard deviations of the two variables are $\bar{x}$ and s_x for the x-values and $\bar{y}$ and s_y for the y-values and n is the number of individual pairs of data. The linear regression, while generally used for prediction of unknown variables, was performed simply to graphically represent the trend on a scatterplot of the two variables.

The square of the correlation coefficient, r^2, or coefficient of variation, was also computed. The coefficient of variation represents the fraction of the variation in one variable that is explained by the regression of the two variables. It provides a means for

comparing the strength of the sunshine/temperature relationship between individual months and sites. Testing of the fit between linear and quadratic relationships was done by comparison of the coefficient of variation from each type of regression. A better quadratic fit highlights potential non-linearity in the relationship between sunshine duration and air temperature.

The annual cycle of the linear correlation coefficients between monthly station air temperature and monthly sunshine duration as a percentage of maximum possible were generated and plotted for each site. This yielded a sequence of twelve coefficients, varying in sign and magnitude for each station that can be compared within the larger dataset.

c) Principal Component Analysis (PCA) or Empirical Orthogonal Function (EOF)

Upon inspection of some of the correlation time series, it was determined that there may be a number of different patterns that could be grouped together. For example, some coastal sites had annual correlation patterns distinctly different from inland sites, and for this reason a principal component analysis (PCA) was performed. PCA is a mathematical manipulation of a dataset covariance matrix for the purpose of identifying patterns in data that explain a sizeable percentage of the total dataset variance. It works by obtaining the eigenvalues and eigenvectors of a covariance matrix, showing how different components of the dataset are oriented in space. The initial result of PCA is the first empirical orthogonal function (EOF) that yields a spatial pattern explaining the largest dataset variance. Often with climatological data, the first EOF can be linked to a known physical process, while subsequent, less prominent patterns, explaining smaller amounts of dataset variance may not be identified with known climatological processes. This is due to the

fact that subsequent EOFs are required to be orthogonal to the first EOF. Generally, atmospheric processes are not orthogonal, but interrelated to some degree.

For this reason, rotation of the EOFs was employed. Rotation was done to enhance the spatial nature of the EOFs in order to produce compact patterns of simple structure by dividing an area into homogeneous sub-areas. In this study, rotation was performed by a technique known as Varimax orthogonal rotation, which follows the idea that when variance is at a maximum, the principal component is most easily interpreted. One of the drawbacks of rotation is that subjective choices must be made about the significance of the EOFs. In this case, rotation was done for three, four, and five principal components. Results obtained by retaining three components were most significant in that the explained variance of each of the components was greater than 5% of the total variance.

The principal component analysis thus produces an unrotated (first) empirical orthogonal function that explains the pattern of highest dataset variance and three rotated principal components that have orthogonal time series and spatially represent simple modes of variability. These three rotated principal components therefore represent annual correlation patterns that are similar across a particular region. PCA also produces what is known as a component loading matrix, which when rescaled gives a -1 to +1 value to each site for each pattern indicating its strength in "belonging to" a particular pattern. High loadings indicate where the locations of high dataset variance occur and describe the degree to which each station is part of the unrotated and rotated patterns. In addition, component scores, which describe the unique temporal variability of each component, are produced. For instances in which a PCA is begun by inputting raw data, rather than the correlations used in this study, scores are time series of a dataset. In this

case, however, the scores represent the orthogonal sequences of twelve correlation coefficients uniquely associated with each spatial pattern of loadings.

4. Results

a) Correlations

Figure 1 presents examples of the shape of common patterns of the correlation coefficient time series. For most of the sites in the study, winter months had negative correlations of weak to moderate strength, and there is a reversal to positive correlations in the spring through the fall. The correlations indicate that relatively low (high) sunshine percentage is associated with relatively high (low) monthly mean air temperatures during the winter months, while the two variables are directly related by the spring season and into the summer and early fall months. The peak of the correlations varies from site to site; many fall near May, others near July, and still others near October (Figure 1).

The sites Fort Wayne, IN and Buffalo, NY (Figures 1a and 1b) show similar October maxima, and Buffalo has a less well-defined springtime correlation peak than is found in Fort Wayne. Philadelphia, PA and Albany, NY annual correlation cycles (Figures 1c and 1d) have well-defined springtime correlation maxima with more variability through the rest of the year. Little Rock, AR and Galveston, TX (Figures 1e and 1f) have springtime correlations lower than the others with slight increases in the fall. The Galveston time series is particularly interesting in that there are no negative correlation values. The sites also show differences in the timing of the fall decline of correlation values. Of the sites shown in Figure 1, three have their first negative value (following the peak correlation) in

the month of November. One is one month prior, one is a month or two later, and one never attains a negative value. In general, most negative correlations occur in or around January. In their study of the relationship between solar irradiance and near-surface temperatures Balling and Roy (2005) determined that on average correlations for any given month are generally higher in strength for coastal sites than those from inland locations. Supporting evidence is provided in Table 2, but for the majority of the correlations produced in this study, the opposite was true. That notwithstanding, it is clear that there is an annual cycle of positive to negative correlation and that one or two clear peaks in correlation can be observed for most sites.

Figure 2 provides two examples of scatterplots of data for all years of record for individual months that have strong positive and negative correlations. The correlation coefficient for Sheridan, WY in October is r = 0.665, indicating a strong positive correlation. In this situation, the trend is upward such that high percentages of sunshine duration indicate high average air temperatures. The opposite situation is shown for Marquette, MI in January where the trend is strongly negative with r = -0.611, indicating that high percentage of sunshine duration is related to relatively low average monthly air temperatures.

b) Principal Component Analysis

As previously noted, a principal component analysis was performed rotating three, four, and five principal components. Keeping in mind that the convention used was to exclude rotated components that explained less than 5% of the variance, it is clear from Table 3 that retaining only three components was of any significance. As expected, the first unrotated component explained most of the variance in the data at 67.5%. By

performing a Varimax rotation PCA on the variance of the first three EOFs, the dataset variance is redistributed to three newly produced rotated component patterns, representing simple spatial data configurations. Following rotation, pattern #1 explained 35.6% of the variance, pattern #2 showed 31.6%, and Pattern #3 showed 17.6% in terms of raw data. When rescaled, the variance explained in each pattern shifts from 58.3% in unrotated #1 to 32.6% in rotated #1, 26.9% in rotated #2, and 16.9% in rotated #3. Overall, these three rotated patterns explain 76.26% of the total rescaled dataset variance.

The spatial loadings of the first unrotated EOF are shown in Figure 3, where each site examined is represented by circles of varying shades and size. As most total data variance is explained by the first unrotated EOF, highest loadings in this pattern show the locations of highest collective variability across the United States, and lower loadings show either less variance or as in the case of negative loadings, locations that have nearly opposite monthly correlation patterns. Thusly, most of the variance is seen to exist in the eastern half of the country with the exception of the southeast coast and in the northwest. Stations in the southwest and the Great Plains are not participating in explaining large amounts of dataset variance. The results suggest that the majority of the sites in the study follow an annual correlation pattern similar to that represented by the first EOF. By looking at the scores (listed in Table 4 and plotted in Figure 4) created for the unrotated pattern #1, the general pattern can be inferred. Negative scores are present for winter months, and positive scores occur in the summer months. It is important to note that these scores are only relative and do not have a direct relationship to the average unrotated pattern #1 sites.

Table 5 shows averaged monthly correlation values for eleven sites with the highest loadings for the unrotated #1 pattern along with the means of those correlation values (Figure 5). Characteristic features of this pattern are a primary spring peak, a secondary October peak, and correlations that generally remain negative from November through February. Again, the lowest negative correlation coefficient value occurs in January. The patterns presented in Figures 4 and 5 do not all match exactly, which is immediately apparent in the case of Spokane, WA, which has only a single peak that occurs in August and others that lack the secondary October peak. Generally, however, the sequences of coefficients are consistently similar among the stations. The reason for this lies in the unusually high loadings that occur in EOF #1. That is, the scores that are presented for the eleven stations in Table 5 are those that do the best at explaining the unrotated #1 pattern.

As previously mentioned, rotation of the first three EOFs resulted in a spatial pattern enhancement providing a representation of three different patterns of monthly correlations across the country. As shown in Table 3, the variance from the unrotated solution shifted and was redistributed among the three rotated solutions. Tables 6-8 show monthly correlation values for the ten sites with the highest loadings for rotated patterns, #1, #2, and #3 along with the means of those values. This information is shown graphically in Figures 6-8.

Each of the patterns has distinctive features. The rotated #1 pattern, which explains 32.6% of the variance, is much like the unrotated #1 pattern with the exception of a well-defined spring peak. There is an even more exaggerated October peak. In addition, correlations for these sites remain positive in November and negative in March, which is

a slight shift compared to the unrotated #1 pattern. One recurring similarity is the January minimum that occurs in most stations of this pattern. The geographical distribution of strong loadings for this pattern is shown in Figure 9. They are grouped mainly in the Midwest and at inland sites in the northeast, but there are also a few stations present in a number of the north-central states, as well. More sites than are depicted fall into the pattern described by the rotated principal component #1, but their loadings fall below the absolute loading value, 0.65.

Rotated pattern #2 is essentially a reverse of the most prominent feature of rotated pattern #1, which is the October peak. The #2 pattern has negative correlations that occur almost collectively in October and even has a few that appear in September, describing an earlier shift to negative correlations than in rotated #1. January is also the month of lowest-value correlations as was the case for unrotated and rotated #1. Overall, the correlation strengths are of lower magnitude than those in other patterns. As shown in Figure 10, sites with strong loadings in this pattern are located primarily in the eastern half of the country clustered along the mid-Atlantic coast extending inland through areas near Tennessee, NM and across the northern edges of the southern states. They generally fall to the immediate south of the sites associated with rotated pattern #1. One outlier is seen in Idaho (Boise), as well.

Rotated pattern #3 is very different from the others, mainly in that the spring correlation peak has been replaced by a sharp peak over the months of June, July, and August. Also of note, the monthly correlations are rarely negative, only frequently having low-magnitude negative values in November and December. In contrast to previous patterns, sites falling under this category have minimum correlation coefficient

values in December rather than in January. Also, though it is not well represented by the mean of these ten sites (Table 8), there is a tendency for sites to have secondary minima in March. The distribution of this pattern shown in Figure 11 leads to the conclusion that this pattern is somehow related to the climate of warm coastal sites as they are clustered near the gulf coast and south-central plains, with one notable outlier on the northern California Pacific coast. Figures 12 and 13 are provided for comparative purposes. Figure 12 shows the mean correlation values at the ten or eleven cities with highest loadings for each unrotated and rotated pattern. Sites not included in Figure 13 do not have strong enough loadings to be deemed significant; this is particularly apparent in the southwestern portion of the country, which appeared in the unrotated results of Figure 3. Interestingly, cities with negative loading values following Varimax rotation with three retained EOFs are concentrated in the southwestern region of the country, appearing to depict another distinct annual pattern of monthly correlation coefficients.

c) Quadratic Regressions

Quadratic regressions were performed on months with high correlation values for sites with high loadings in each of the rotated patterns in order to determine if a quadratic relationship was a better fit to the data than linear regression. The comparison (Table 9) was performed for peak correlation months (associated with peaks in the annual cycle of a particular rotated pattern) having linear correlations greater than r = 0.3 among the 30 sites (Tables 6-8) that made up the top ten highest rotated loadings. Evaluation of the regression result was made in terms of the difference in the coefficients of variation, r^2. The largest difference occurred in Nashville, TN in January, where a quadratic function explains 18.9% more variance between sunshine duration percentage and average

monthly air temperature in that month than a linear correlation. This value is unusually large in comparison with the data sampled; all other sites showed much less improvement in the percentage of explained variation (Figure 14). For all but three of those sites, a quadratic curve fit the data better than a linear relation to some extent, and in the case of the three where a linear regression provided a better fit to the data, the differences for two of these three are essentially negligible. Table 9 shows these two difference values to greater than four decimal places, as rounding would make them equal to zero at that point.

Also of interest was the sign of the quadratic regression coefficient, *a*, which determines whether the curve is concave up or concave down. Figures 15-20 are quadratic regression scatterplots for months that are representative of their associated rotated pattern and that have a significantly better fit to a quadratic function. Figures 15 and 16 show Alpena, MI in October and Williston, ND in August, representative peak correlation months for rotated pattern #1. Each quadratic function explains about 3% more variance than a linear function. In the case of the linear regressions, both have positive relationships; however the curve for Alpena is concave up, while the curve for Williston is concave down. This indicates that both relatively low and high percentages of sunshine duration are indicative of higher temperatures in October in Alpena, and the situation is the opposite for Williston in August. The quadratic regression for Nashville in April and Memphis, TN in June, representative months of rotated pattern #2, explain 7.4% and 6.8%, respectively, more total variance than a linear function (Figures 17 and 18). Signs of *a* are also opposite in this situation. The quadratic regression for Oklahoma City, OK in June and Miami, FL in August, representative months of rotated pattern #3,

explain 7.8% and 4.1%, respectively, more total variance than a linear function (Figures 19 and 20). Signs of *a* are both positive (concave up) in this situation, but this is not representative of all rotated pattern #3 representative months, as shown in Table 9.

Given this information, it does not appear that there is much uniformity in the signs of the x^2-coefficient among all sites or even sites of one particular pattern. In addition, the magnitude of this coefficient must also be taken into consideration because as it approaches zero, the quadratic regression curve looks more and more like a straight line, and therefore any difference in correlation coefficients should be insignificant. In addition, Nashville in January (rotated pattern #2, non-representative month) and Sheridan in November (rotated pattern #1, non-representative but high linear correlation month) had the greatest magnitude values for *a* of 0.0207 and 0.0134, respectively (Figures 21 and 22). Both are concave up, meaning both low and high values of sunshine duration percentage indicate relatively higher average monthly air temperatures. One final detail to note is that for many sites, such as Oklahoma City in June and Miami in August (Figures 19 and 20), there are sunshine duration percentage values that do not appear in the dataset that would be useful in providing supporting evidence for a better quadratic fit. For example, for Miami in August, sunshine duration percentages do not have values much less than 50%, which corresponds with a critical point on the quadratic curve, where lower sunshine duration percentages may be associated with higher average monthly air temperatures. This association (or lack thereof) cannot be known without a significant decline in monthly sunshine duration percentages over Miami in August at some point in time.

5. Discussion and Conclusions

The results of this study may have applications in a few areas of the atmospheric sciences. Overall, it has been shown that the relationship between average monthly sunshine duration percentage and average monthly air temperatures varies in both time and space in an organized, patterned fashion. Therefore, it should be beneficial to take this spatial and temporal pattern into consideration when using temperature and radiation parameters to study weather and climate.

Since Angell *et al.* (1984) found that "for the contiguous United States, the correlation between year-average values of cloudiness and sunshine has been -0.92," the generalization can be made that high values of sunshine duration percentage can also be read as low values of cloudiness. Therefore, the results of this study are directly applicable to weather forecasting in the United States, because correct forecasting of cloud cover has a direct link to the correct forecasting of temperatures. It is known that the cloud cover has more of an effect on air temperatures in certain months rather than others; this is often the case in the Midwest during the spring where a great deal of clouds can mean much cooler air temperatures. Figures 5-7 show that many areas have high correlation coefficients during the spring months, depicting the strong relationship that is weaker in the summer. This relationship is important to understand when forecasting for multiple regions of the country. For instance, the correlations are not as strong in southeastern states in the spring, but they are some of the strongest nationwide during the summer months. There is also a very clear difference in the relationship during October for rotated pattern #1 and #2 cities, which would be beneficial to understand while forecasting for cities in both areas. It would be important to know when the relationship

switches from positive to negative or negative to positive for a particular area, as well. Taking these annual cycles of correlation coefficients into account should result in improved forecasts, at least to some degree.

These results may also be applied to radiation parameterizations in many kinds of models, as the relatively small effect this relationship may have on model predictions may accumulate error over different regions. Since clouds and radiation are parameterized rather than being precise representations, this small-scale interaction should aid in improving their representations and the effects that they have on temperature values produced by the models.

The spatial and temporal patterns of correlation coefficients between monthly average sunshine duration percentage and average monthly air temperature duration produced during this study may also have use in climate change research. A number of studies have reported on the observed decrease in solar radiation at the Earth's surface on the order of 6 to 9 W m^{-2} occurring from roughly 1960 to 1990, a phenomenon known as global dimming (Wild *et al.* 2005; Farquhar and Roderick 2003; Pinker *et al.* 2005; Stanhill and Cohen 2001). The reduction is believed to have been caused by large amounts of atmospheric pollutants, aerosols, and dust and has noted influences on multiple environmental processes, such as changing surface temperature and even increasing photosynthetic productivity in plants due to their affinity for diffuse light (Farquhar and Roderick 2003). After 1990, however, global dimming has changed into global brightening (Wild *et al.* 2005; Pinker *et al.* 2005), as anti-pollution legislation, such as the United States' 1990 Clean Air Act, went into effect and the collapse of communist economies caused a reduction in industrial pollutants (Schiermeier 2005).

The problem is that some scientists believe the dust and aerosols may have been protecting the planet from enhanced effects of global warming. If that is truly the case, questions arise as to how additional solar irradiance is going to affect temperatures in the future. This uncertainty is complicated by the fact that the response of temperature may differ regionally. Understanding of the regional patterns of the radiation/temperature relationship may be able to ease the complication and allow for better prediction of how temperatures will change regionally and seasonally with increases in radiation and sunshine duration percentage.

In terms of future related analysis, it would be beneficial to learn more about the possible quadratic nature of the relationship between monthly average sunshine duration percentage and monthly average air temperatures by looking at both larger geographical areas and different time scales, as well as annual cycles of monthly quadratic correlation values. Currently there is work being done involving analysis of linear and quadratic regressions between daily air temperature and solar radiation divided and averaged into thirty-six ten-day periods over a smaller region. Preliminary results have shown, as was the case here, a better fit of the data to a quadratic function than to a linear function. Further, the results show x^2-coefficients that are predominantly negative, indicating some cohesive pattern. In addition, annual linear and quadratic correlation patterns should be created and analyzed for a greater number of locations around the globe in an attempt to find similar patterns that can be mapped on a larger scale. In doing this, time should be taken to research other atmospheric processes that have influences on these patterns, such as the seasonal shifting of the polar and subtropical jets, changes in humidity, or simple environmental features that are specific to certain locations. From this, it may be

determined that these relationship features are inherent to any region at a more elemental level, possibly acting as a method to characterize regions climatologically.

Acknowledgements:

I would like to thank my advisor, Jeff Rogers, for making every aspect of this project possible by providing data, guidance, and answers when I needed them. I would also like to thank Andrew Annunzio for his assistance in understanding the mathematics behind some of the analysis and Jay Hobgood and Richard Yerkes for acting as members of my reviewing committee.

References:

Angell, J.K., *et al*., 1984: Variation in United Stated cloudiness and sunshine, 1950-82. *Journal of Climate and Applied Meteorology*, 23: 752-761.

Balling, R.C., and S.S. Roy, 2005: Analysis of spatial patterns underlying the linkage between solar irradiance and near-surface air temperatures. *Geophysical Research Letters*, 32: L11702.

Farquhar, G.D., and M.L. Roderick, 2003: Pinatubo, diffuse light, and the carbon cycle. *Science*, 299: 1997-1998.

Gleisner, H., and P. Thejil, 2003: Patterns of tropospheric response to solar variability. *Geophysical Research Letters*, 30(13): 1711.

Meehl, G.A., *et al.*, 2003: Solar and greenhouse gas forcing and climate response in the twentieth century. *Journal of Climate*, 16: 426-444.

Moore & McCabe, 2006: Introduction to the Practice of Statistics (5^{th} ed.). New York: W.H. Freeman & Company: 123-151.

Pinker, R.T., B. Zhang, and E.G. Dutton, 2005: Do satellites detect trends in surface solar radiation. *Science*, 308: 850-854.

Quinlan, F.T., 1985: A history of sunshine data in the United States. Handbook of Applied Meteorology, D.D. Houghton (Ed), New York: John Wiley & Sons: 1199-1201.

Rodionov, S., 2004: A sequential algorithm for testing climate regime shifts. *Geophysical Research Letters*, 31: doi: 10.1029/2004GL019448.

Schiermeier, Q., 2005: Cleaner skies leave global warming forecasts uncertain. *Nature,* 435: 135.

Stanhill, G., and S. Cohen, 2001: Global dimming: A review of the evidence for a widespread and significant reduction in global radiation with discussion of its probable causes and possible agricultural consequences. *Agricultural and Forest Meteorology*, 107: 255-278.

Stanhill, G., and S. Cohen, 2005: Solar radiation changes in the United States during the twentieth century: Evidence from sunshine duration measurements. *Journal of Climate*, 18: 1503-1512.

Steurer, P.M., and T.R. Karl, 1991: Historical sunshine and cloud data in the United States. Environmental Sciences Division Publication 3689, CDIAC-43, Oak Ridge National Laboratory, 98 pp.

Wild, M., *et al.*, 2005: From dimming to brightening: Decadal changes in solar radiation at Earth's surface. *Science*, 203: 847-850.

List of Tables

List of Figures

Table 1. List of the 113 sites analyzed in this study along with their beginning year of comparison. Data comparison ranged from the year listed to 1987 in all cases.

Site	Earliest Year of Comparison	Site	Earliest Year of Comparison	Site	Earliest Year of Comparison
Albany	1939	Grand Junction	1901	Pittsburgh	1926
Albuquerque	1897	Grand Rapids	1948	Pocatello	1939
Alpena	1918	Green Bay	1902	Portland, ME	1920
Amarillo	1948	Greenville	1930	Portland, OR	1929
Apalachicola	1931	Harrisburg	1926	Providence	1949
Ashville	1947	Hartford	1920	Pueblo	1948
Atlanta	1930	Havre	1905	Raleigh	1949
Atlantic City	1949	Helena	1894	Rapid City	1948
Baltimore	1894	Houston	1946	Richmond	1949
Binghamton	1952	Huron	1948	Rochester	1926
Birmingham	1930	Indianapolis	1897	Roswell	1905
Bismark	1948	Jacksonville	1944	Salt Lake City	1948
Boise	1940	Kansas City	1949	San Antonio	1947
Boston	1920	Key West	1949	San Diego	1927
Brownsville	1923	Knoxville	1911	San Francisco	1948
Buffalo	1922	Lander	1949	Sault Sainte Marie	1931
Burlington	1920	Lansing	1948	Seattle	1948
Charleston	1930	Little Rock	1897	Sheridan	1949
Charlotte	1919	Los Angeles	1945	Sioux City	1908
Chattanooga	1928	Louisville	1895	Spokane	1897
Cheyenne	1915	Lynchburg	1930	Springfield, IL	1902
Chicago	1896	Macon	1949	Springfield, MO	1915
Cleveland	1897	Madison	1905	St. Louis	1948
Columbia	1898	Marquette	1948	Tampa	1933
Columbus	1897	Memphis	1928	Toledo	1900
Concordia	1949	Miami	1948	Topeka	1949
Covington	1947	Milford	1928	Walla Walla	1931
Dayton	1913	Milwaukee	1902	Washington D.C.	1949
Denver	1949	Minneapolis	1897	Wichita	1949
Des Moines	1896	Missoula	1949	Williston	1948
Detroit	1948	Nashville	1948	Wilmington	1933
Dodge City	1949	New Orleans	1930	Winnemucca	1928
El Paso	1948	New York City	1898	Yuma	1908
Elkins	1926	Norfolk	1949		
Eureka	1948	North Platte	1948		
Evansville	1913	Oklahoma City	1948		
Fort Smith	1905	Omaha	1955		
Fort Wayne	1913	Parkersburg	1926		
Fresno	1948	Peoria	1906		
Galveston	1947	Philadelphia	1926		

Table 2. Annual cycles of correlation coefficients between average monthly sunshine duration percentage of maximum and average monthly air temperatures for select coastal and inland locations.

	Coastal Sites			Inland Sites		
	Key_West	**Portland_OR**	**Seattle**	**Green_Bay**	**St_Louis**	**Yuma**
J	0.3730536	-0.3352786	-0.2732739	-0.481288	0.0032476	0.1481454
F	0.3195986	0.2519604	0.159455	-0.3407845	0.1524342	0.0579177
M	0.5155084	0.3456696	0.1777548	-0.0246274	0.3060941	0.1665202
A	0.0586767	0.3414695	0.2561692	0.4163096	0.3298357	0.2841679
M	0.3879249	0.4080926	0.5266305	0.1936936	0.3773998	0.2140181
J	0.4032954	0.5465218	0.6396996	0.18726	0.3314057	-0.1219641
J	0.3771806	0.6633539	0.6683549	0.3878866	0.2316132	0.0797
A	-0.020866	0.6028158	0.5410028	0.2797827	0.2391392	0.1349931
S	0.350435	0.5627572	0.5070087	0.241599	0.3410257	0.2166481
O	0.2096271	0.3546967	0.3910442	0.4131117	0.0416008	0.1399741
N	0.1923539	-0.2732331	-0.142074	-0.0481135	0.147246	0.1097852
D	0.1091292	-0.375552	-0.2659386	-0.2011786	-0.1522826	0.3022116

Table 3. The total variance explained by principal component analysis, including variance explained following rotation of the first three EOFs and initial eigenvalues. Variance was computed for all 113 possible components, but only the top eleven are shown as the rest were insignificant. Values are shown in raw and rescaled quantities.

Component	Initial Eigenvalues			Extraction Sums of Squared Loadings			Rotation Sums of Squared Loadings		
Raw	Total	% of Variance	Cumulative %	Total	% of Variance	Cumulative %	Total	% of Variance	Cumulative %
1	5.148	67.542	67.542	5.148	67.542	67.542	2.715	35.62	35.62
2	0.917	12.035	79.577	0.917	12.035	79.577	2.406	31.57	67.19
3	0.398	5.218	84.795	0.398	5.218	84.795	1.342	17.605	84.795
4	0.258	3.387	88.182						
5	0.193	2.538	90.719						
6	0.175	2.302	93.021						
7	0.146	1.918	94.939						
8	0.11	1.437	96.377						
9	0.106	1.392	97.769						
10	0.088	1.159	98.928						
11	0.082	1.072	100						
...									
Rescaled	Total	% of Variance	Cumulative %	Total	% of Variance	Cumulative %	Total	% of Variance	Cumulative %
1	5.148	67.542	67.542	65.873	58.295	58.295	36.786	32.554	32.554
2	0.917	12.035	79.577	13.635	12.066	70.361	30.346	26.855	59.409
3	0.398	5.218	84.795	6.666	5.899	76.26	19.042	16.851	76.26
4	0.258	3.387	88.182						
5	0.193	2.538	90.719						
6	0.175	2.302	93.021						
7	0.146	1.918	94.939						
8	0.11	1.437	96.377						
9	0.106	1.392	97.769						
10	0.088	1.159	98.928						
11	0.082	1.072	100						
...									

Table 4. Scores generated by principal component analysis for each month in the unrotated #1 pattern.

Month	Scores
January	-1.73363
February	-1.08408
March	-0.12817
April	0.87734
May	0.87302
June	1.068
July	0.95886
August	0.65104
September	0.51012
October	0.11143
November	-0.66385
December	-1.44005

Table 5. Annual cycles of correlation coefficients between average monthly sunshine duration percentage of maximum and average monthly air temperatures for the eleven sites with highest loadings for the unrotated #1 pattern following principal component analysis. The means of these values are also included.

	Albany	Boston	Evansville	Fort Wayne	Hartford	Indianapolis
J	-0.5097218	-0.2619727	-0.2726241	-0.48997	-0.4211166	-0.2957877
F	-0.3333284	-0.1961641	-0.1213577	-0.33893	-0.1656943	-0.1282209
M	-0.1093526	0.1102588	0.2058052	0.14222	-0.0270077	0.1472908
A	0.3772487	0.3071145	0.4033455	0.4288	0.248129	0.4416369
M	0.5618141	0.5355689	0.5212388	0.43649	0.4595967	0.482283
J	0.4096072	0.6184291	0.3748039	0.44837	0.326036	0.5577959
J	0.2544104	0.4543712	0.2690042	0.35103	0.3618659	0.3613801
A	0.2404623	0.3078589	0.2860303	0.2469	0.1293491	0.2271896
S	0.158816	0.3547046	0.187522	0.13917	0.1488122	0.232899
O	0.2210377	0.4192586	0.1992608	0.30977	-0.0040701	0.3778868
N	-0.0691805	0.0907373	0.1460437	-0.04277	-0.0861301	-0.0175396
D	-0.5869175	-0.1248021	-0.2310248	-0.24971	-0.3731437	-0.2429897
	Milwuakee	**Peoria**	**Providence**	**Spokane**	**Toledo**	**Mean**
J	-0.3947729	-0.2344589	-0.4450919	-0.3361398	-0.2762608	-0.357992473
F	-0.2974832	-0.210042	-0.3505054	-0.0519184	-0.2155553	-0.219018155
M	0.1705671	0.2274038	0.0117989	0.1849171	0.1983056	0.114746091
A	0.3415263	0.540001	0.3374162	0.4873694	0.5028256	0.401401191
M	0.2678288	0.5422498	0.5056735	0.5658209	0.4343781	0.482994782
J	0.4551857	0.5224212	0.4335651	0.540792	0.501493	0.471681736
J	0.4719163	0.4687774	0.4902629	0.6142089	0.5051534	0.418398245
A	0.3067964	0.3684508	0.3436409	0.6620435	0.3380418	0.314251236
S	0.2783964	0.2244019	0.2896774	0.5925332	0.2340596	0.258272027
O	0.4773144	0.3359182	-0.1486463	0.3650657	0.3846863	0.267043827
N	-0.0413615	-0.0463239	-0.1284957	-0.1696327	-0.0632808	-0.038903073
D	-0.3331282	-0.1965271	-0.3392537	-0.4269688	-0.2632312	-0.306154255

Table 6. Annual cycles of correlation coefficients between average monthly sunshine duration percentage of maximum and average monthly air temperatures for the ten sites with highest loadings for the rotated #1 pattern following principal component analysis. The means of these values are also included.

	Alpena	Bismark	Buffalo	Burlington	Marquette	
J	-0.4411408	-0.2451013	-0.1693335	-0.5161448	-0.6107952	
F	-0.4528467	-0.2700917	-0.0929702	-0.4320548	-0.2746988	
M	-0.1220992	0.0996648	-0.0206353	-0.3995772	-0.3414076	
A	0.1720763	0.6662056	0.3172798	0.1856841	0.2593935	
M	0.3047059	0.2779516	0.227926	0.3848692	0.4553282	
J	0.1344441	0.5757716	0.3565465	0.2924021	0.2253245	
J	0.2509085	0.0367439	0.2611856	0.1799012	0.3644519	
A	0.1920018	0.5353179	0.3744814	0.1631712	0.1543421	
S	0.2449387	0.6019133	0.2929782	0.1236978	0.2793512	
O	0.5449853	0.6068703	0.5500035	0.3548829	0.5334349	
N	0.0872794	0.2482771	0.034065	0.0364871	0.0536469	
D	-0.1673639	0.124252	0.0065998	-0.4025495	-0.3390137	
	Minneapolis	**Rochester**	**Sault Sainte Marie**	**Sheridan**	**Williston**	**Mean**
J	-0.2493615	-0.2585922	-0.581314	0.1764822	-0.0679467	-0.29632478
F	-0.1604328	-0.2798271	-0.416836	0.211958	-0.1787822	-0.23465823
M	0.2084209	-0.0239682	-0.076649	0.0377544	0.1773251	-0.04611713
A	0.5209001	0.3619041	0.182271	0.673261	0.5868009	0.39257764
M	0.4015241	0.3482176	0.235266	0.4462309	0.3783487	0.34603682
J	0.5356802	0.3121632	0.265447	0.6947182	0.4512969	0.38437943
J	0.5235229	0.2999875	0.38896	0.3594577	0.2433327	0.29084519
A	0.2388718	0.322058	0.375865	0.3687358	0.6158726	0.33407176
S	0.458306	0.2516861	0.24103	0.6739998	0.7058018	0.38737029
O	0.4845925	0.534955	0.519436	0.6653373	0.5659242	0.53604219
N	0.2891925	0.0348692	0.02576	0.4595722	0.3504812	0.16196306
D	0.0068228	-0.2569257	-0.301918	0.1282159	0.0302817	-0.11715986

Table 7. The same as Table 6 but for the rotated #2 pattern.

	Harrisburg	Knoxville	Memphis	Nashville	Norfolk	
J	-0.4701677	-0.3670564	-0.3387869	-0.3633549	-0.2925837	
F	-0.3372761	-0.0319528	0.0791687	-0.1074152	-0.1070911	
M	0.1353199	0.0889178	0.2858458	0.3067747	0.0631138	
A	0.3421317	0.3408975	0.3529638	0.4355673	0.4628746	
M	0.5562617	0.3363926	0.1717395	0.221143	0.3188235	
J	0.2327384	0.3940368	0.4780125	0.3022117	0.2289939	
J	0.3607714	0.3870718	0.367139	0.3723659	0.3164496	
A	0.3081941	0.2441597	0.2726815	0.2314179	0.0545371	
S	0.2310152	0.1552919	0.1735469	0.1353538	-0.0441889	
O	-0.1520545	-0.1455512	-0.068526	-0.2160053	-0.4586304	
N	-0.1301332	0.0134636	-0.0295075	-0.304065	-0.2837782	
D	-0.3021179	-0.0473145	-0.1756098	-0.3170683	-0.4441462	
	Philadelphia	**Raleigh**	**St. Louis**	**Washington DC**	**Wilmington**	**Mean**
J	-0.3808481	-0.4685282	0.0032476	-0.4448783	-0.3446212	-0.34675778
F	-0.0324502	-0.4028721	0.1524342	0.0776818	-0.1848117	-0.08945845
M	0.203883	0.0655088	0.3060941	0.1801652	0.1182178	0.17538409
A	0.3757198	0.2248484	0.3298357	0.5142152	0.2039905	0.35830445
M	0.4984687	0.1148032	0.3773998	0.4724819	0.2222782	0.32897921
J	0.3189929	0.3413055	0.3314057	0.4677368	0.2331125	0.33285467
J	0.3523169	0.3813433	0.2316132	0.3664381	0.4056949	0.35412041
A	0.0863915	0.2330469	0.2391392	0.1916917	0.1549694	0.2016229
S	0.183545	0.0458204	0.3410257	0.3618457	0.0573869	0.16406426
O	-0.2172518	-0.3455792	0.0416008	-0.4411301	-0.2897247	-0.22928524
N	-0.1549949	-0.3866156	0.147246	-0.2284446	-0.1047073	-0.14615367
D	-0.3506446	-0.3970844	-0.1522826	-0.6029077	-0.0337743	-0.28229503

Table 8. The same as Table 6 but for the rotated #3 pattern.

	Apalachicola	Galveston	Houston	Little Rock	Macon	
J	0.0508911	0.1171469	0.0269166	-0.2301809	-0.2901815	
F	-0.0412201	0.2409899	0.010898	0.0176706	-0.0263553	
M	0.0743881	0.0925859	-0.0693357	0.2263422	0.1171367	
A	0.0055183	0.2290491	0.1020728	0.164836	0.0004148	
M	0.0015218	0.1261194	-0.2441928	0.1707592	0.3262541	
J	0.2207263	0.3191644	0.3081748	0.4670606	0.4453523	
J	0.2861731	0.4929322	0.6739497	0.4766337	0.4700704	
A	0.3981986	0.4927287	0.681502	0.5192255	0.605929	
S	0.293974	0.4159445	0.1733489	0.2533014	0.1322781	
O	-0.0250236	0.0876023	-0.2473553	0.0798602	-0.3007115	
N	-0.0988863	0.1202317	-0.0887871	-0.1142204	-0.3504796	
D	-0.1942991	0.1396316	-0.1968958	-0.2056003	-0.2501572	
	Miami	New Orleans	Oklahoma City	San Antonio	Wichita	Mean
J	0.0697783	-0.2064314	0.330272	0.1953521	0.456975	0.05205382
F	0.3733654	-0.0906273	0.529556	0.2211336	0.564013	0.17994238
M	0.0457822	-0.0227158	0.496345	0.0422981	0.45264	0.14554667
A	-0.0224137	-0.1653646	0.423626	-0.0404014	0.314216	0.10115533
M	0.014857	0.1794513	0.191435	0.3459528	0.054141	0.11662988
J	0.5315299	0.3186868	0.565595	0.4564287	0.484528	0.41172468
J	0.5925093	0.3414982	0.598878	0.7537594	0.689083	0.5375487
A	0.35012	0.4023508	0.536004	0.6190829	0.646505	0.52516465
S	0.2735913	0.1434171	0.493133	0.1522642	0.482083	0.28133355
O	0.093885	-0.0411839	0.38271	-0.0103718	0.511559	0.05309704
N	0.1056311	-0.0919014	0.099353	0.0022555	0.141689	-0.02751145
D	-0.3010769	-0.1012001	0.051392	-0.1037615	0.042533	-0.11194343

Table 9. Results of the comparison of the coefficients of variation resultant from linear and quadratic regression analyses performed on the sites listed in Tables 6-8. Results are ordered by the magnitude of the quadratic minus the linear coefficients of variation from greatest to least.

PATTERN	CITY	MONTH	r	LINEAR r^2	QUADRATIC r^2	QUAD - LIN	x^2 Coefficient
2	**Nashville**	January	-0.3634	0.1320	0.3207	0.1887	0.0134
2	**Norfolk**	October	-0.4586	0.2103	0.3264	0.1161	0.0050
1	**Sheridan**	November	0.4596	0.2112	0.3244	0.1132	0.0207
3	**Oklahoma City**	June	0.5656	0.3199	0.3978	0.0779	0.0086
3	**Oklahoma City**	February	0.5296	0.2804	0.3568	0.0764	0.0071
2	**Nashville**	April	0.4356	0.1897	0.2639	0.0742	-0.0071
2	**Memphis**	June	0.4780	0.2285	0.2966	0.0681	0.0051
3	**Wichita**	September	0.4821	0.2324	0.2865	0.0541	0.0035
1	**Williston**	June	0.4513	0.2037	0.2561	0.0524	0.0101
2	**Raleigh**	October	-0.3456	0.1194	0.1655	0.0461	0.0048
2	**St. Louis**	September	0.3410	0.1163	0.1617	0.0454	0.0041
2	**Raleigh**	November	-0.3866	0.1495	0.1929	0.0434	0.0030
1	**Rochester**	May	0.3481	0.1212	0.1645	0.0433	0.0051
3	**Miami**	August	0.3501	0.1226	0.1632	0.0406	0.0024
3	**Wichita**	January	0.4570	0.2088	0.2468	0.0380	0.0044
3	**Wichita**	February	0.5640	0.3181	0.3543	0.0362	0.0057
3	**Macon**	July	0.4701	0.2210	0.2529	0.0319	-0.0022
1	**Williston**	August	0.6159	0.3793	0.4107	0.0314	-0.0068
1	**Alpena**	October	0.5450	0.2970	0.3283	0.0313	0.0025
3	**New Orleans**	August	0.4024	0.1619	0.1911	0.0292	0.0026
3	**Little Rock**	June	0.4671	0.2181	0.2471	0.0290	0.0036
3	**Miami**	June	0.5315	0.2825	0.3089	0.0264	0.0016
1	**Sheridan**	April	0.6733	0.4533	0.4794	0.0261	0.0039
2	**Wilmington**	January	-0.3446	0.1188	0.1447	0.0259	0.0078
2	**Norfolk**	December	-0.4442	0.1973	0.2230	0.0257	-0.0058
1	**Bismark**	September	0.6019	0.3623	0.3880	0.0257	-0.0032
2	**Washington D.C.**	June	0.4677	0.2188	0.2434	0.0246	-0.0039
1	**Bismark**	August	0.5353	0.2866	0.3099	0.0233	-0.0050
1	**Burlington**	May	0.3849	0.1481	0.1697	0.0216	-0.0034
1	**Bismark**	October	0.6069	0.3683	0.3898	0.0215	0.0025
1	**Minneapolis**	May	0.4015	0.1612	0.1826	0.0214	0.0037
2	**Knoxville**	May	0.3364	0.1132	0.1327	0.0195	0.0043
3	**Wichita**	March	0.4526	0.2049	0.2242	0.0193	0.0037
1	**Marquette**	October	0.5334	0.2846	0.3034	0.0188	0.0030
2	**Norfolk**	April	0.4629	0.2143	0.2325	0.0182	0.0033
3	**Houston**	August	0.6815	0.4644	0.4820	0.0176	0.0014
3	**San Antonio**	August	0.6191	0.3833	0.4004	0.0171	0.0019
1	**Williston**	October	0.5659	0.3203	0.3372	0.0169	-0.0028
3	**Galveston**	September	0.4159	0.1730	0.1898	0.0168	-0.0017
3	**Miami**	July	0.5925	0.3511	0.3671	0.0160	0.0009
1	**Bismark**	April	0.6662	0.4438	0.4592	0.0154	0.0027
3	**New Orleans**	June	0.3187	0.1016	0.1155	0.0139	0.0015
3	**Oklahoma City**	August	0.5360	0.2873	0.3012	0.0139	0.0042
1	**Sault Sainte Marie**	February	-0.4168	0.1738	0.1872	0.0134	0.0069

3	**New Orleans**	July	0.3415	0.1166	0.1299	0.0133	0.0014
1	**Williston**	April	0.5868	0.3443	0.3572	0.0129	0.0017
1	**Rochester**	October	0.5350	0.2862	0.2986	0.0124	0.0025
2	**Nashville**	July	0.3724	0.1387	0.1502	0.0115	0.0019
2	**St. Louis**	April	0.3298	0.1088	0.1200	0.0112	-0.0023
1	**Minneapolis**	July	0.5235	0.2741	0.2852	0.0111	0.0025
3	**Houston**	July	0.6740	0.4542	0.4648	0.0106	0.0009
2	**Norfolk**	May	0.3188	0.1016	0.1112	0.0096	0.0021
2	**Philadelphia**	April	0.3757	0.1412	0.1506	0.0094	0.0003
2	**Washington D.C.**	December	-0.6029	0.3635	0.3726	0.0091	-0.0038
1	**Sheridan**	October	0.6653	0.4427	0.4513	0.0086	-0.0030
3	**Oklahoma City**	April	0.4236	0.1795	0.1877	0.0082	0.0018
2	**Philadelphia**	January	-0.3809	0.1450	0.1525	0.0075	0.0039
2	**Wilmington**	July	0.4057	0.1646	0.1720	0.0074	0.0014
2	**Harrisburg**	July	0.3608	0.1302	0.1374	0.0072	0.0014
3	**Oklahoma City**	March	0.4963	0.2464	0.2532	0.0068	-0.0021
3	**Oklahoma City**	July	0.5989	0.3587	0.3649	0.0062	0.0016
2	**Raleigh**	February	-0.4029	0.1623	0.1684	0.0061	0.0022
3	**Miami**	February	0.3734	0.1394	0.1440	0.0046	0.0019
3	**Apalachicola**	September	0.2940	0.0864	0.0910	0.0046	-0.0006
3	**Little Rock**	July	0.4766	0.2272	0.2314	0.0042	0.0009
1	**Buffalo**	August	0.3745	0.1402	0.1444	0.0042	0.0016
2	**Knoxville**	April	0.3409	0.1162	0.1203	0.0041	0.0011
2	**Philadelphia**	December	-0.3506	0.1229	0.1267	0.0038	-0.0021
1	**Sault Sainte Marie**	October	0.5194	0.2698	0.2734	0.0036	0.0012
2	**Washington D.C.**	May	0.4725	0.2232	0.2265	0.0033	0.0025
2	**Harrisburg**	January	-0.4702	0.2211	0.2243	0.0032	0.0016
1	**Sheridan**	May	0.4462	0.1991	0.2022	0.0031	0.0016
3	**Little Rock**	August	0.5193	0.2696	0.2727	0.0031	-0.0010
1	**Buffalo**	October	0.5500	0.3025	0.3055	0.0030	0.0010
1	**Alpena**	February	-0.4529	0.2051	0.2080	0.0029	-0.0024
1	**Burlington**	February	-0.4321	0.1867	0.1894	0.0027	-0.0029
2	**St. Louis**	May	0.3774	0.1424	0.1449	0.0025	0.0014
1	**Sault Sainte Marie**	January	-0.5813	0.3379	0.3403	0.0024	0.0026
1	**Burlington**	October	0.3549	0.1259	0.1283	0.0024	0.0009
1	**Minneapolis**	September	0.4583	0.2100	0.2121	0.0021	-0.0008
2	**Knoxville**	June	0.3940	0.1553	0.1573	0.0020	0.0006
1	**Marquette**	May	0.4553	0.2073	0.2092	0.0019	0.0010
1	**Sheridan**	September	0.6740	0.4543	0.4559	0.0016	-0.0011
3	**Wichita**	August	0.6465	0.4180	0.4195	0.0015	0.0020
3	**Galveston**	August	0.4927	0.2428	0.2443	0.0015	0.0004
3	**Apalachicola**	August	0.3982	0.1586	0.1596	0.0010	0.0002
3	**Wichita**	June	0.4845	0.2348	0.2358	0.0010	-0.0009
2	**Memphis**	April	0.3530	0.1246	0.1255	0.0009	-0.0008
1	**Williston**	September	0.7058	0.4982	0.4990	0.0008	-0.0006
3	**Apalachicola**	July	0.2862	0.0819	0.0826	0.0007	-0.0002
3	**Wichita**	July	0.6891	0.4748	0.4755	0.0007	0.0007
1	**Minneapolis**	April	0.5209	0.2713	0.2719	0.0006	0.0006
2	**Washington D.C.**	April	0.5142	0.2644	0.2649	0.0005	-0.0003
2	**Raleigh**	December	-0.3971	0.1577	0.1581	0.0004	-0.0005

2	**Knoxville**	July	0.3871	0.1498	0.1502	0.0004	0.0003
2	**Philadelphia**	May	0.4985	0.2485	0.2488	0.0003	0.0004
1	**Burlington**	January	-0.5161	0.2664	0.2667	0.0003	-0.0007
3	**Macon**	August	0.6059	0.3671	0.3674	0.0003	0.0002
3	**Galveston**	July	0.4929	0.2430	0.2432	0.0002	-0.0001
2	**Harrisburg**	May	0.5563	0.3094	0.3096	0.0002	-0.0003
3	**Macon**	June	0.4454	0.1983	0.1985	0.0002	-0.0002
3	**San Antonio**	July	0.7538	0.5682	0.5683	0.0001	0.0001
1	**Minneapolis**	June	0.5357	0.2870	0.2871	0.0001	-0.0003
1	**Buffalo**	April	0.3173	0.1007	0.1008	0.0001	0.0003
1	**Rochester**	April	0.3619	0.1310	0.1311	0.0001	0.0003
2	**Raleigh**	January	-0.4685	0.2195	0.2195	-0.00002	0.000002
1	**Buffalo**	June	0.3565	0.1271	0.1271	-0.00003	-0.0001
1	**Marquette**	January	-0.6108	0.3731	0.2166	-0.1565	-0.0378

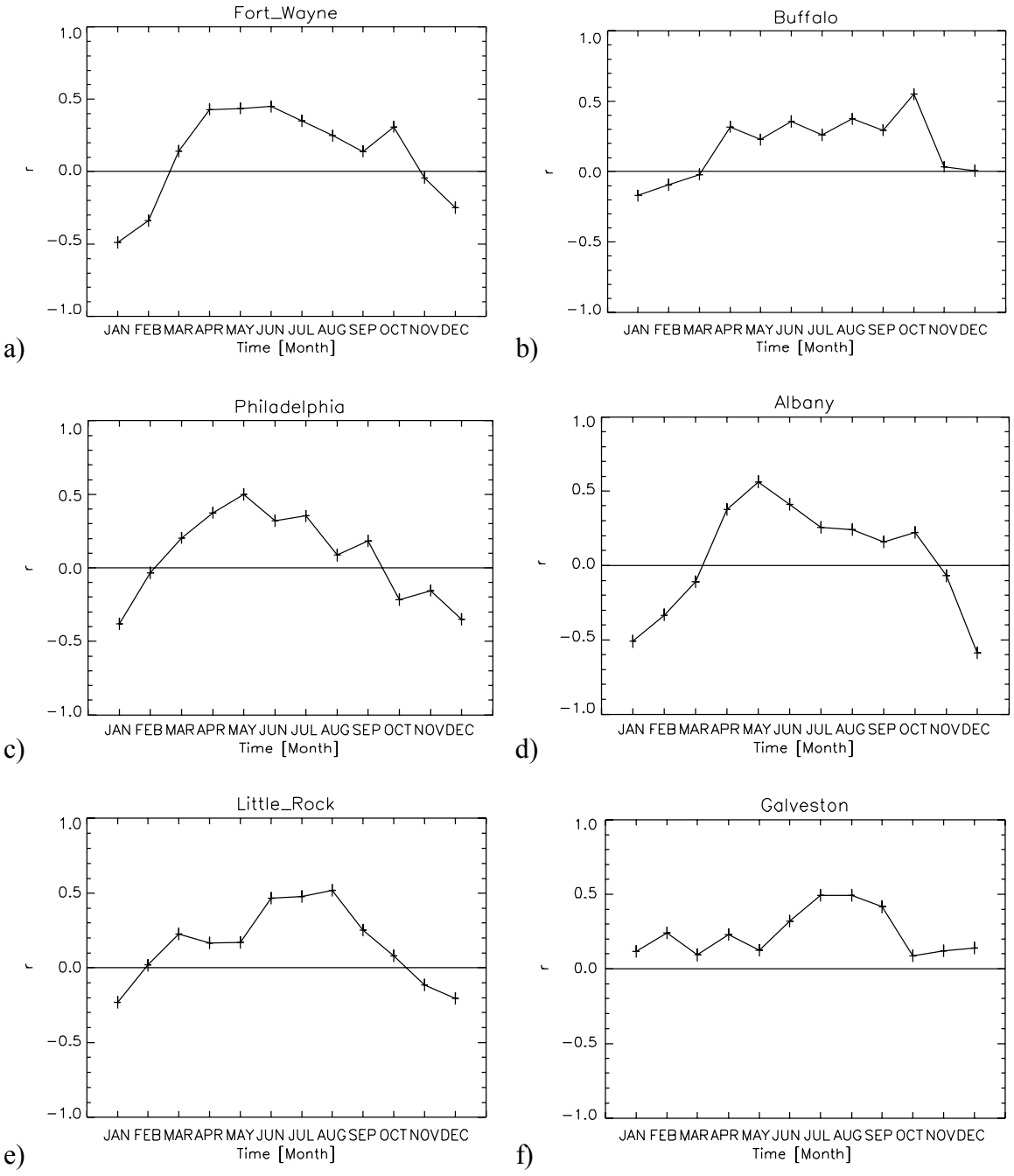

Figure 1. Annual cycles of correlation coefficients between average monthly sunshine duration percentage of maximum and average monthly air temperatures for six selected sites.

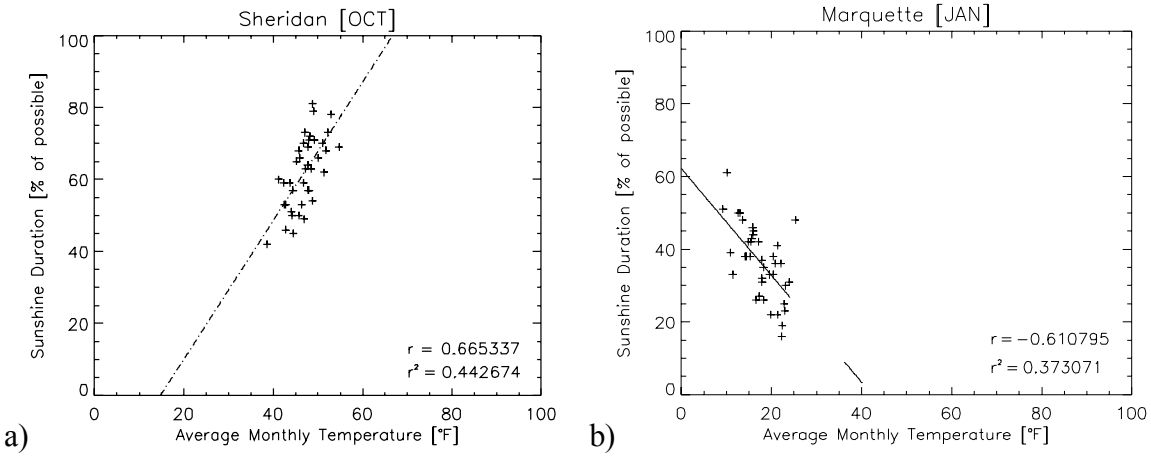

Figure 2. Scatterplots of average monthly air temperature versus average monthly sunshine duration percentage of maximum possible with plotted linear regression lines, correlation coefficients and coefficients of variation.

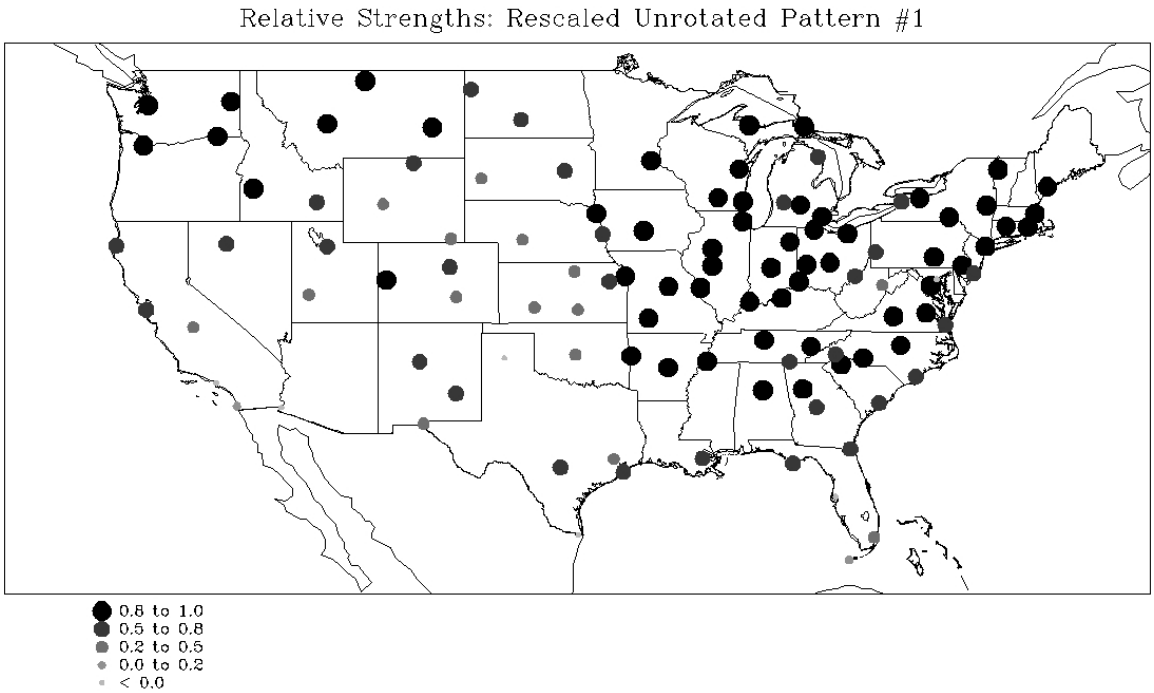

Figure 3. Spatial loadings of the first unrotated EOF. All sites examined in this study are shown.

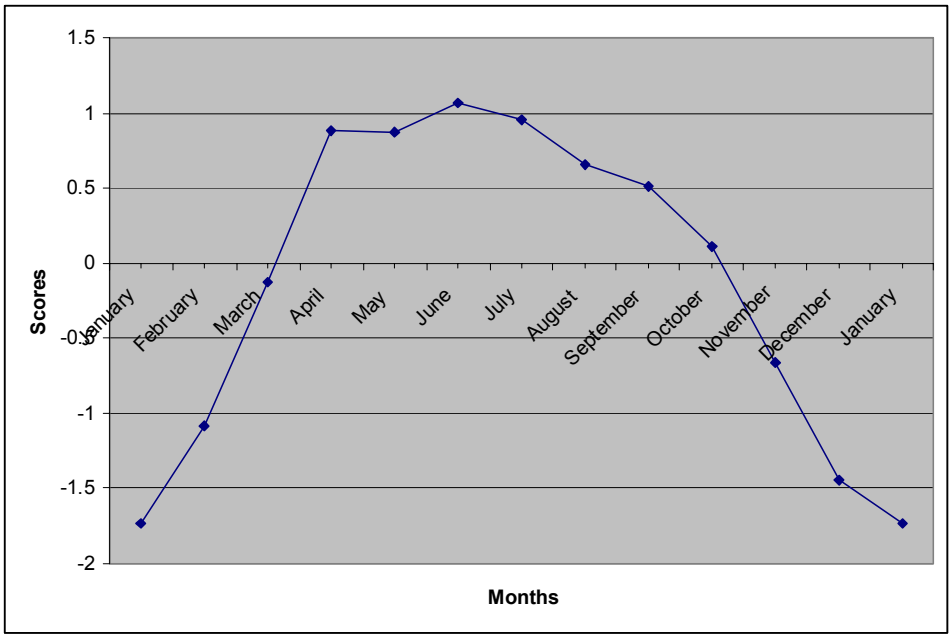

Figure 4. Scores generated by principal component analysis for each month in the unrotated #1 pattern.

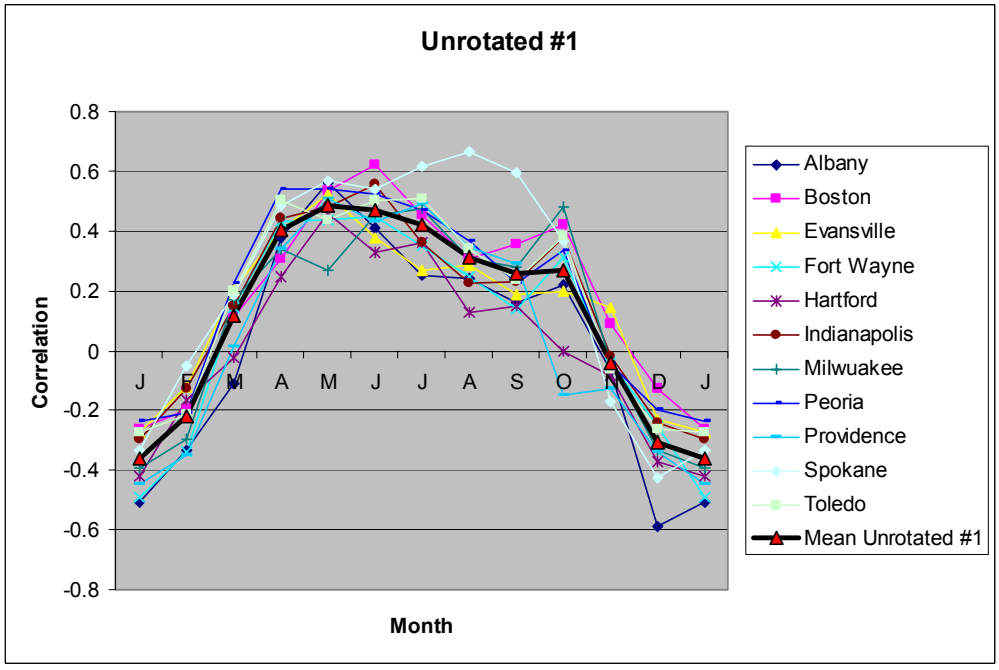

Figure 5. Annual cycles of correlation coefficients between average monthly sunshine duration percentage of maximum and average monthly air temperatures for the eleven sites with highest loadings for the unrotated #1 pattern following principal component analysis. The means of these values are also plotted.

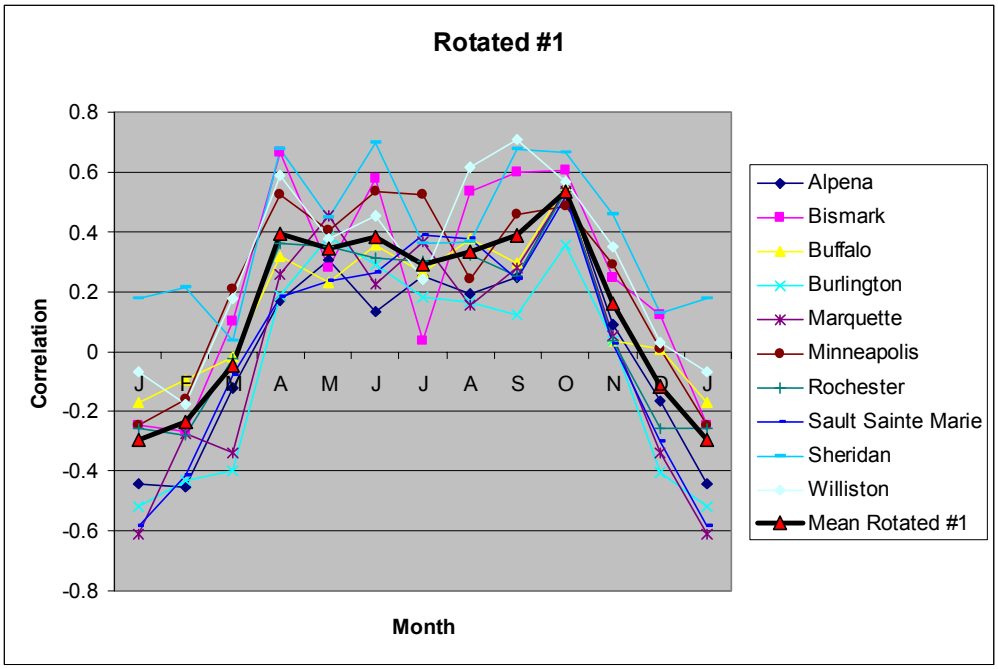

Figure 6. Annual cycles of correlation coefficients between average monthly sunshine duration percentage of maximum and average monthly air temperatures for the ten sites with highest loadings for the rotated #1 pattern following principal component analysis. The means of these values are also plotted.

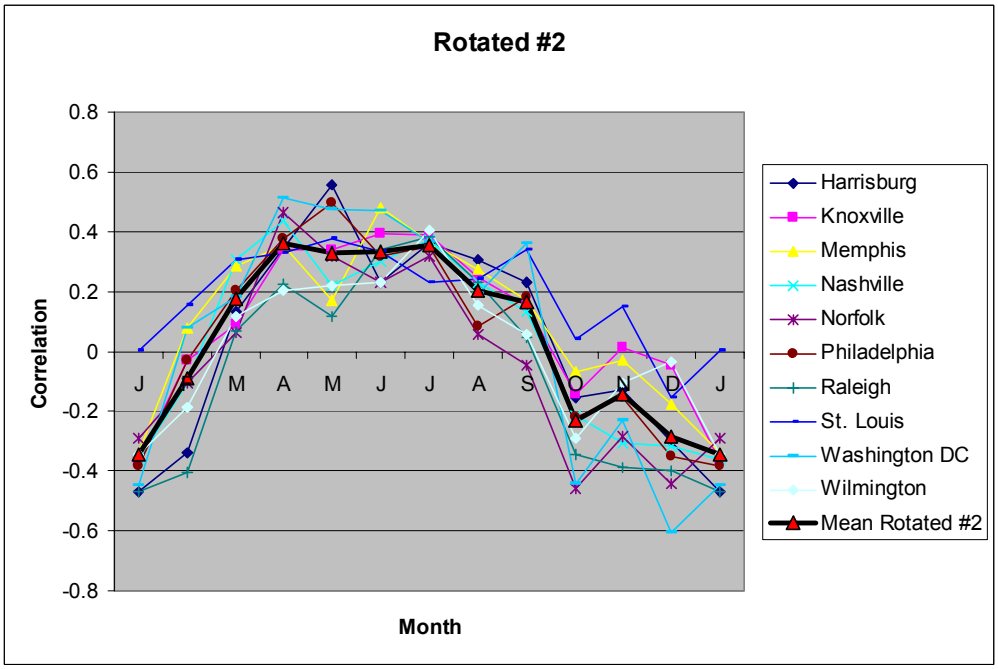

Figure 7. Same as Figure 6 but for the rotated #2 pattern.

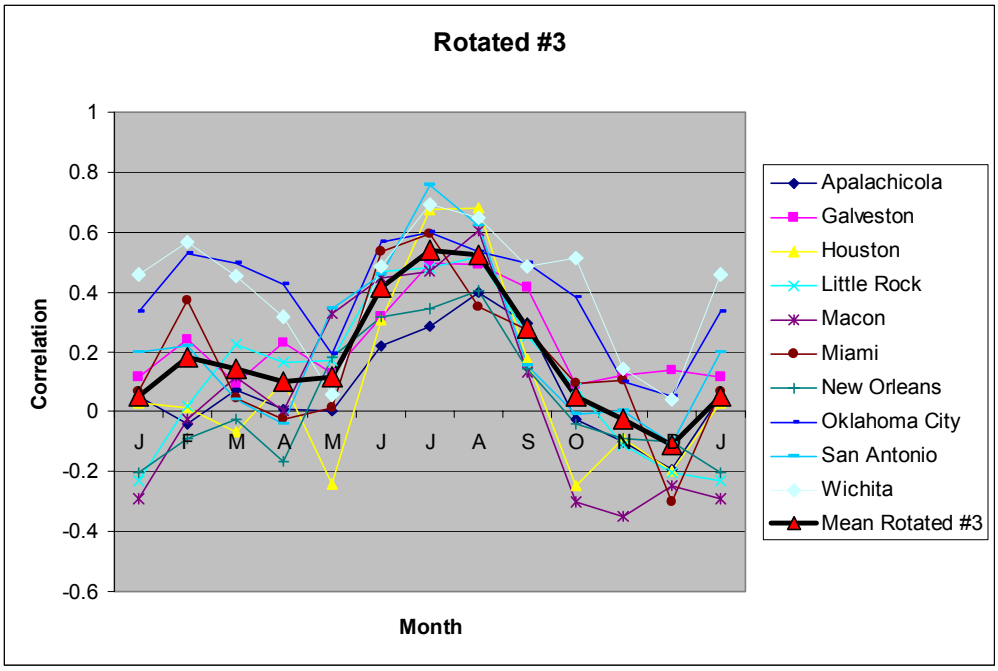

Figure 8. Same as Figure 6 but for the rotated #2 pattern.

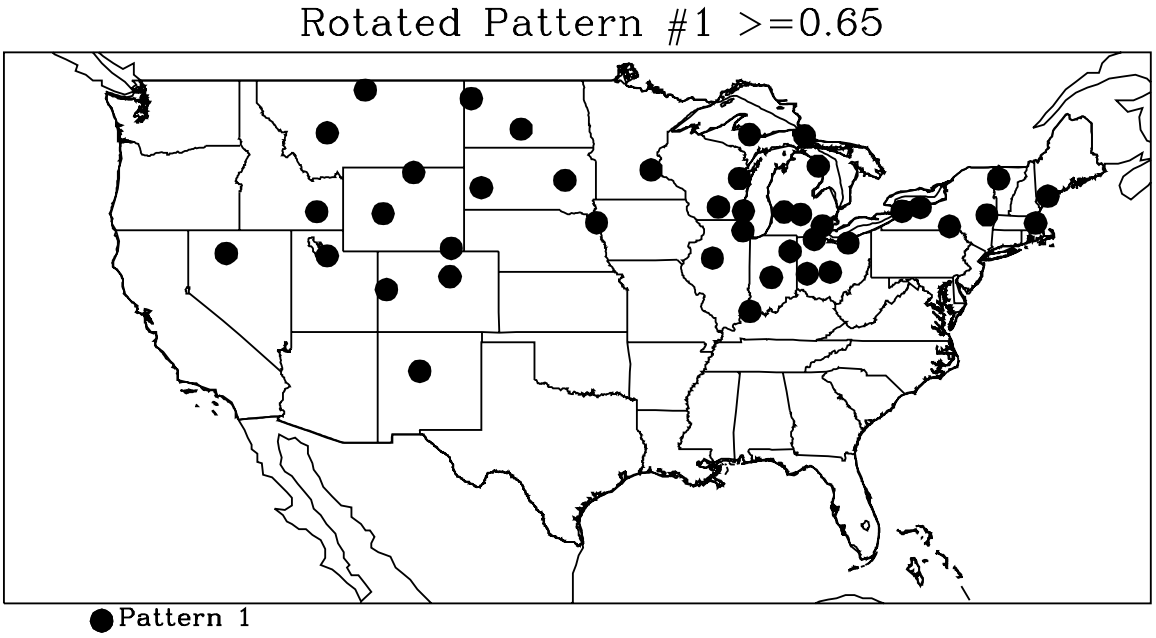

Figure 9. Rotated principal component #1 of the annual cycle of monthly correlations between average monthly sunshine duration percentage of maximum and average monthly air temperatures. The dots indicate the stations having loading values above 0.65 for component #1.

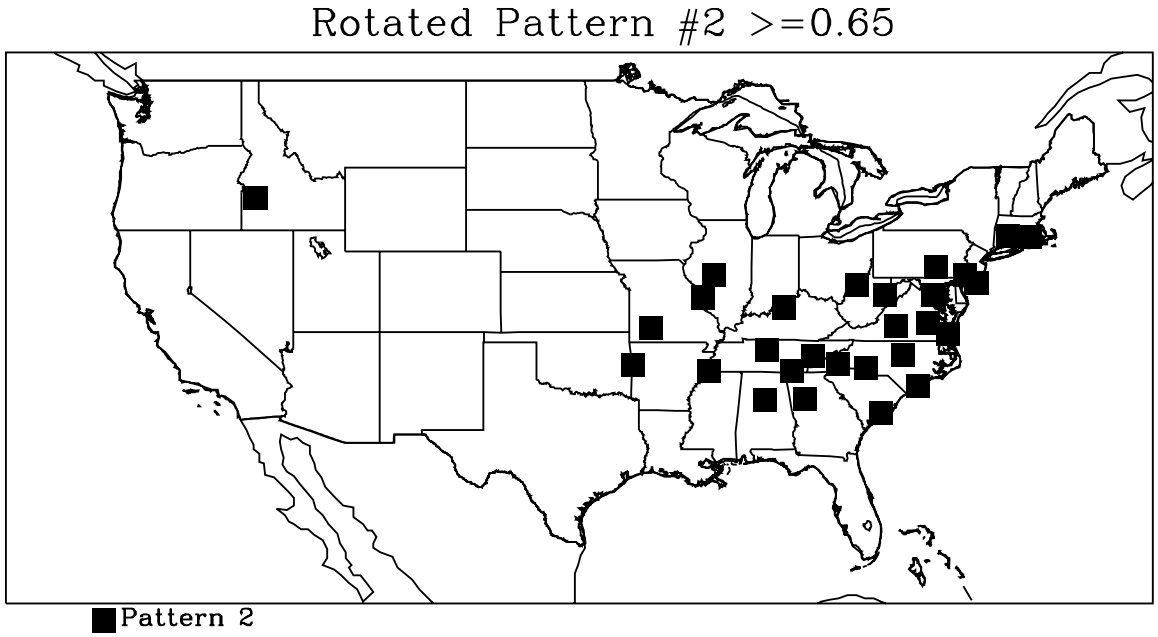

Figure 10. Same as Figure 10 but for rotated principal component #2.

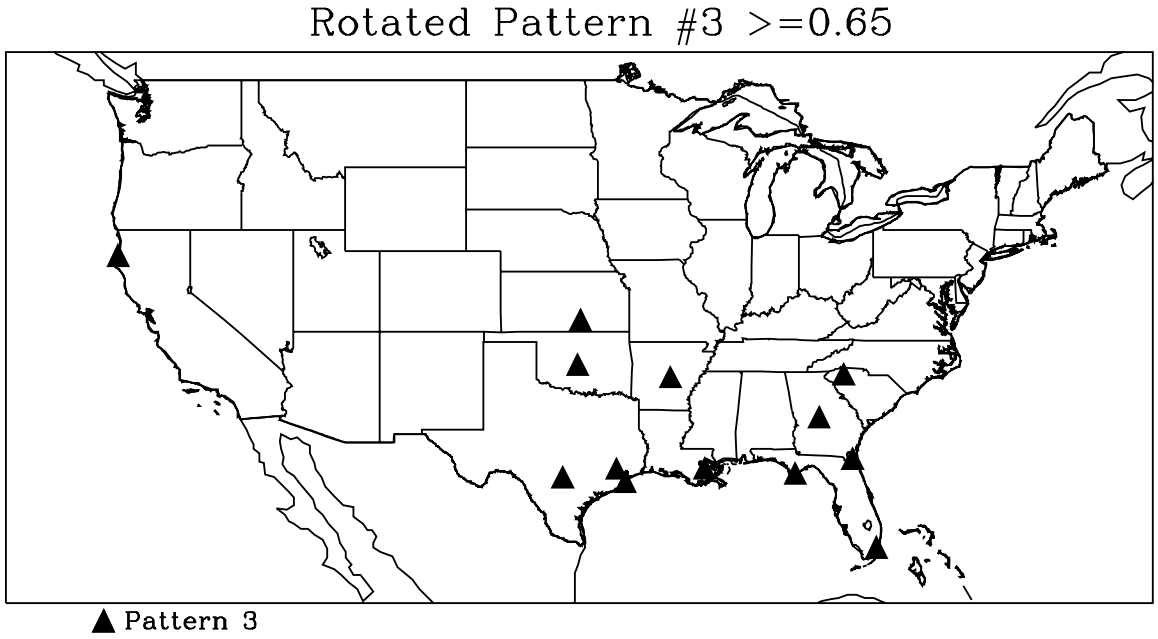

Figure 11. Same as Figure 10 but for rotated principal component #3.

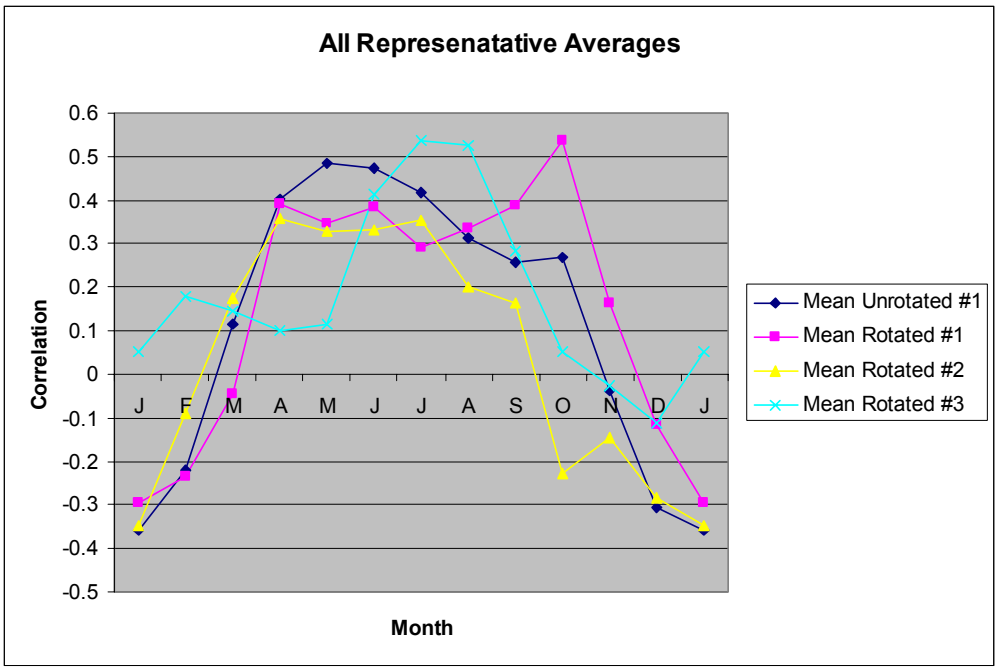

Figure 12. The mean monthly correlation values between average monthly sunshine duration percentage of maximum and average monthly air temperatures for the sites listed in Tables 5-8, showing unrotated pattern #1 and rotated patterns #1-3.

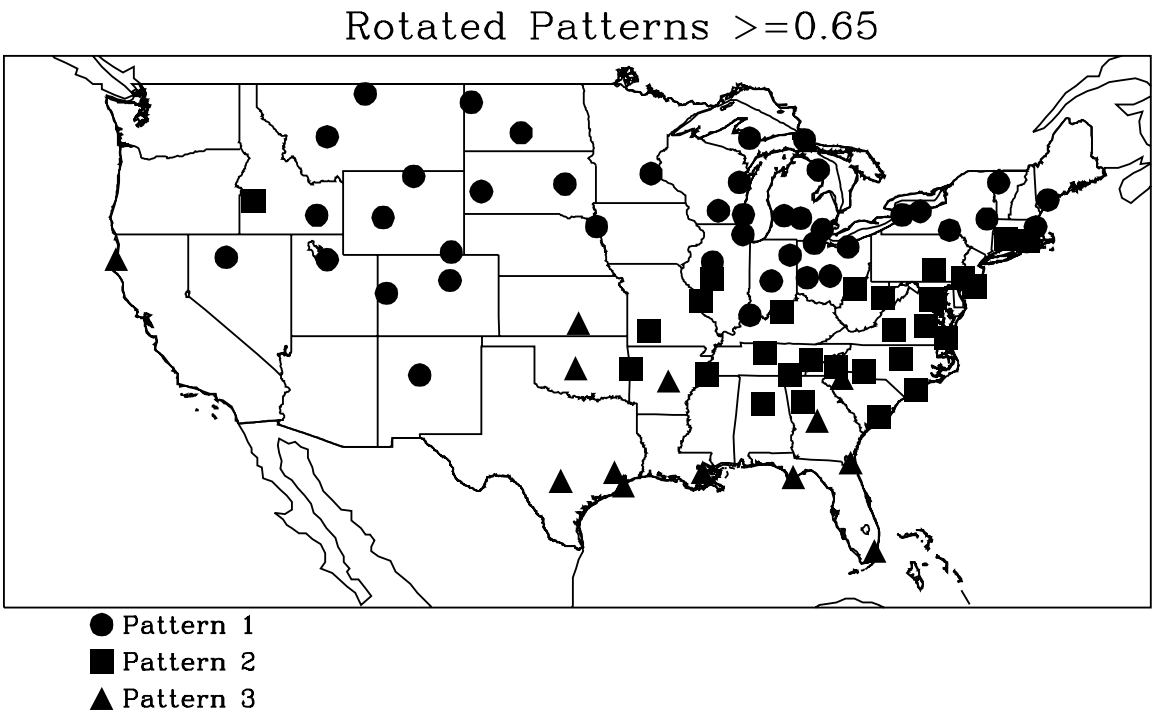

Figure 13. The same as Figures 9-11 but for all three rotated principal components.

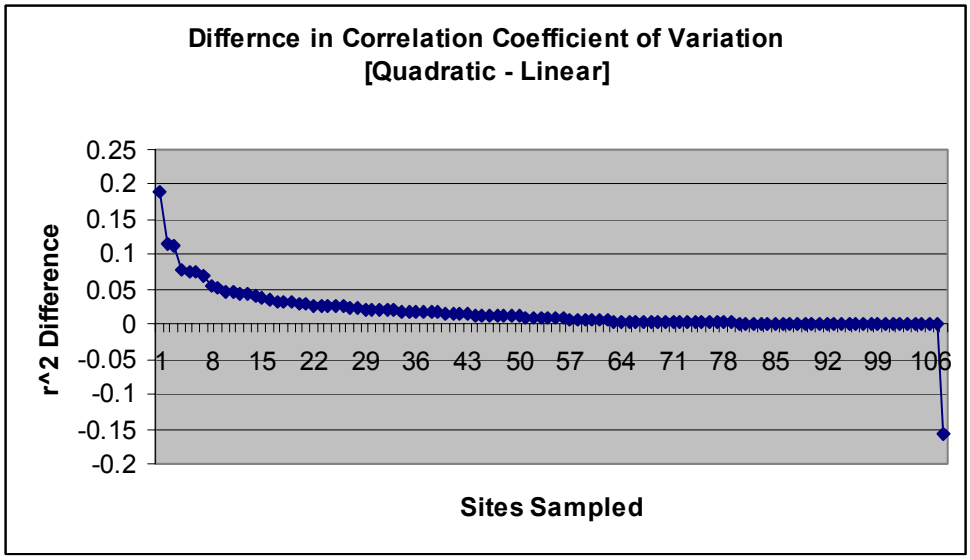

Figure 14. Plot of the difference values, quadratic minus linear coefficients of variation, as listed in Table 9.

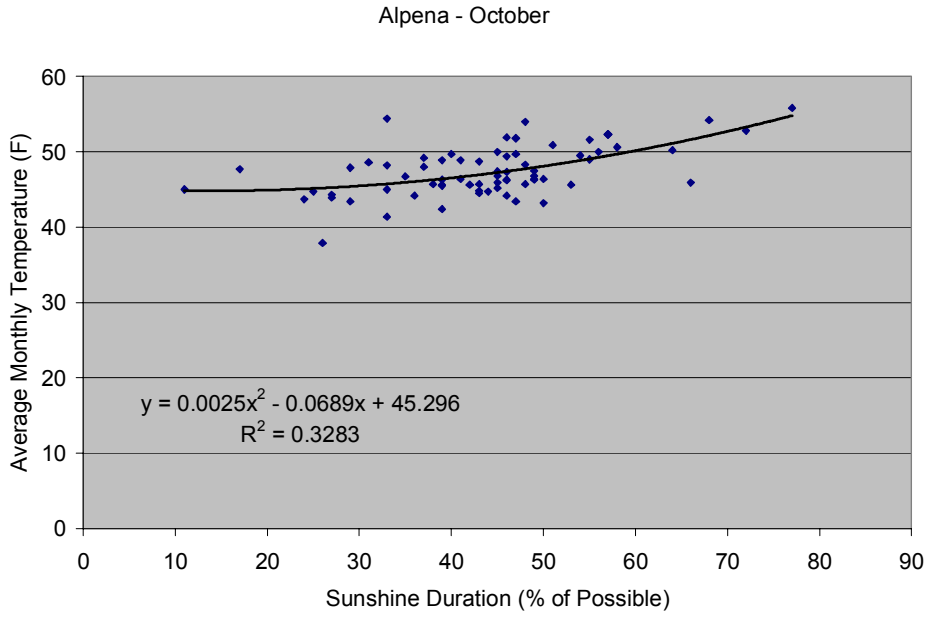

Figure 15. Scatterplots of sunshine duration percentage of maximum possible versus average monthly air temperature with plotted quadratic regression line for Alpena in October. The coefficient of variation and equation of the quadratic curve are also shown.

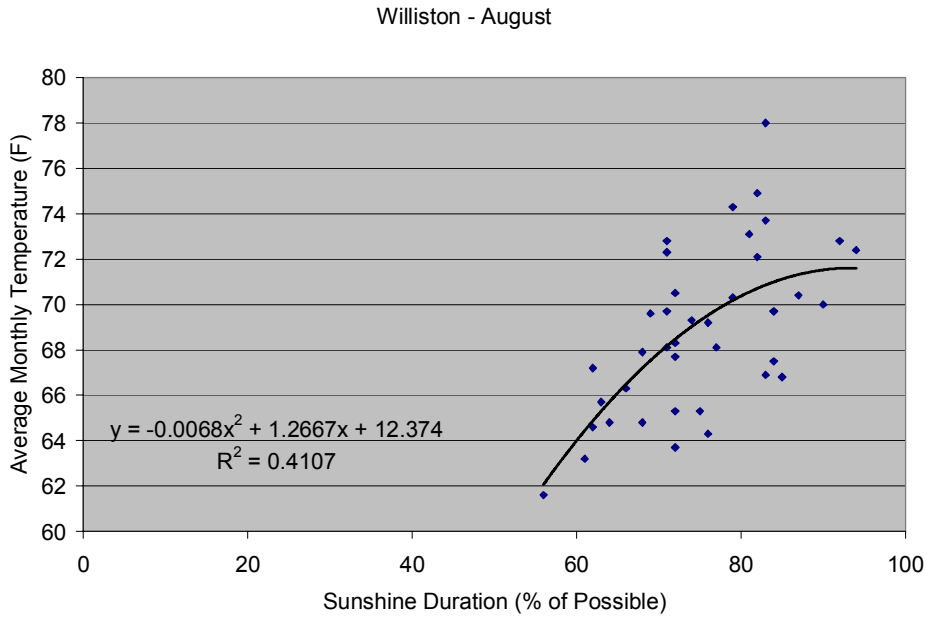

Figure 16. Same as Figure 15 but for Williston in August.

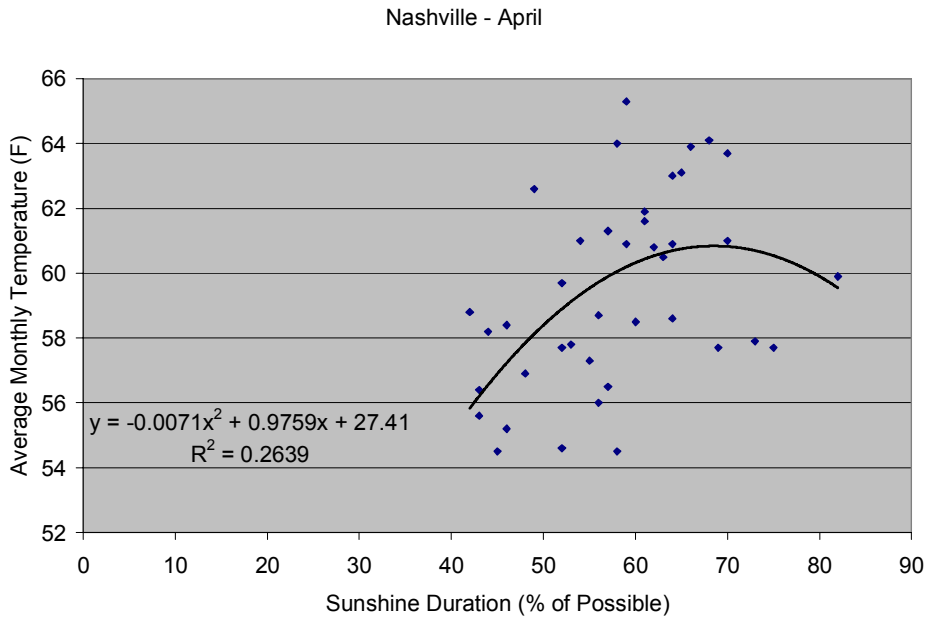

Figure 17. Same as Figure 15 but for Nashville in April.

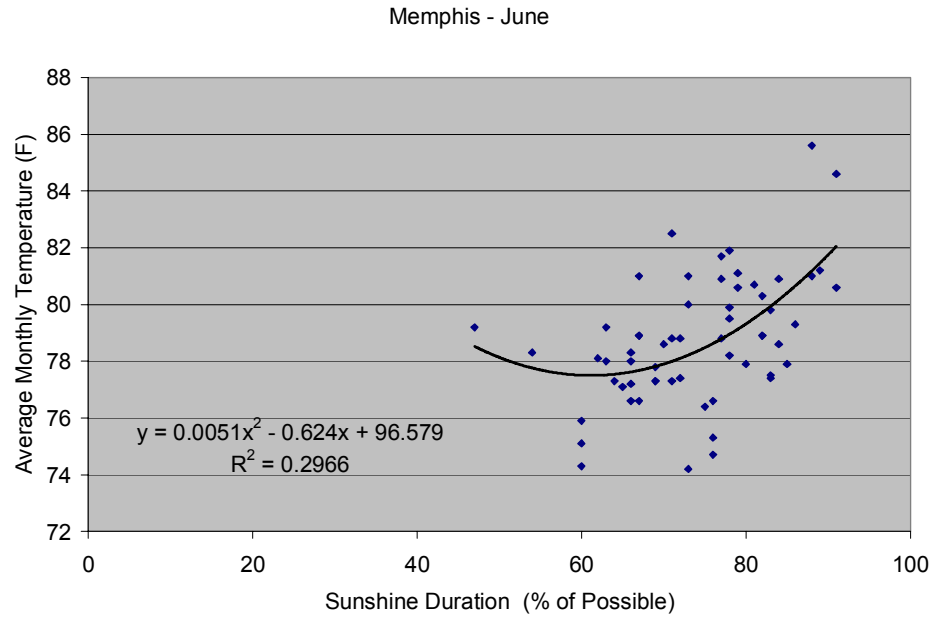

Figure 18. Same as Figure 15 but for Memphis in June.

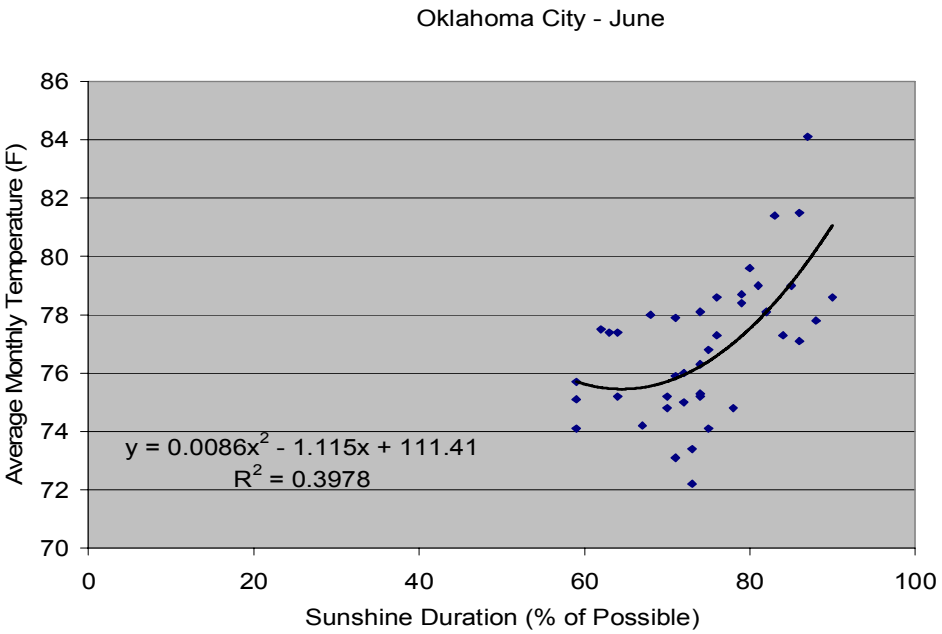

Figure 19. Same as Figure 15 but for Oklahoma City in June.

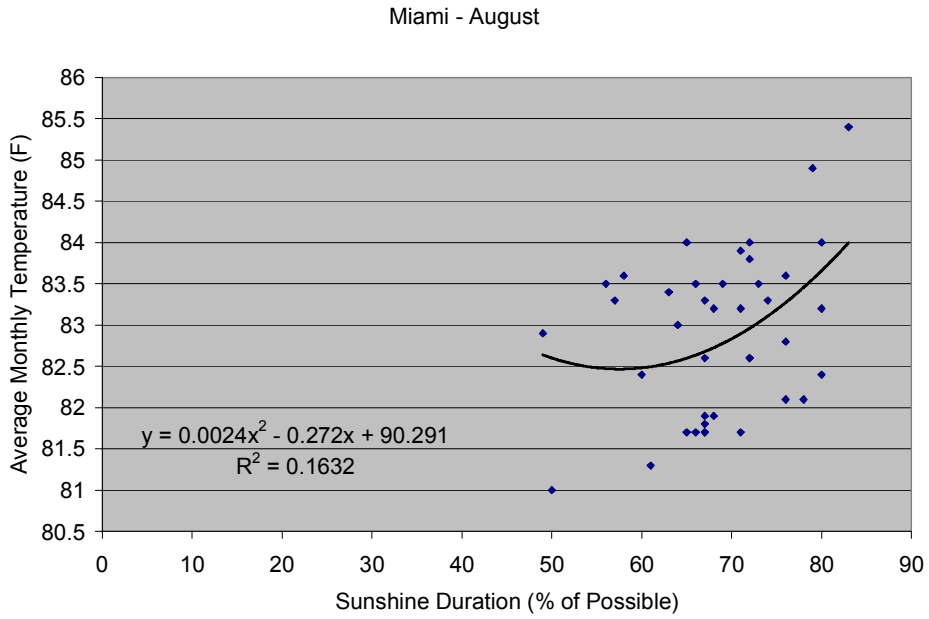

Figure 20. Same as Figure 15 but for Miami in August.

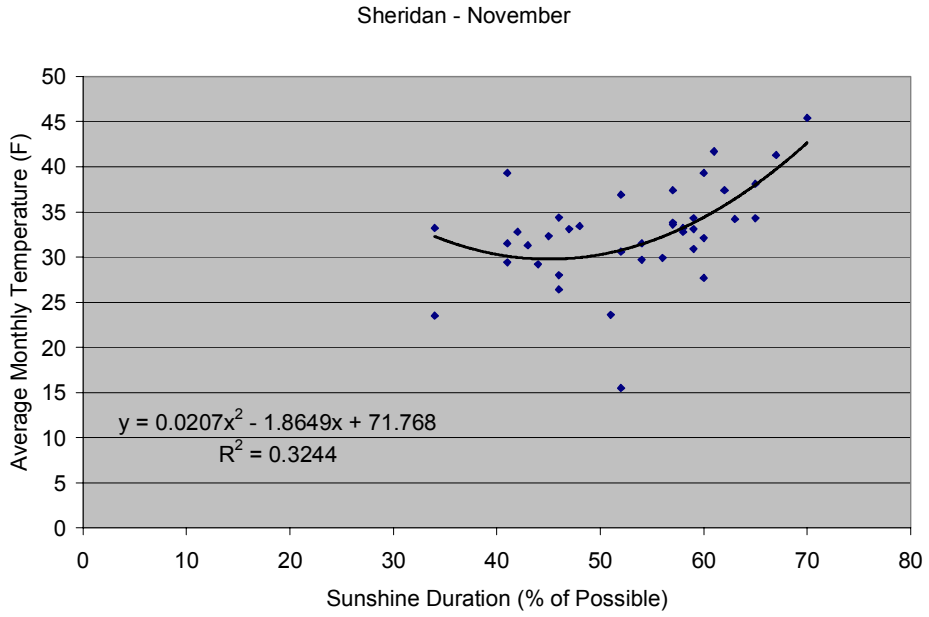

Figure 21. Same as Figure 15 but for Sheridan in November.

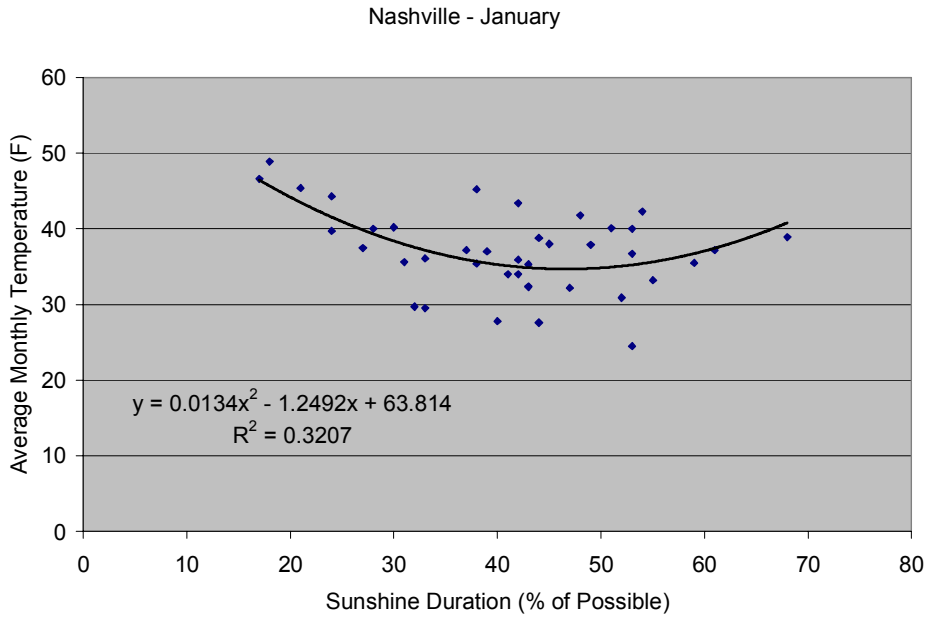

Figure 22. Same as Figure 15 but for Nashville in January.